View metadata, citation and similar papers at core.ac.uk
brought to you by CORE
provided by Royal Holloway - Pure

Taphonomic and zooarchaeological investigations at the middle Pleistocene site of Ti's al Ghadah, western Nefud Desert, Saudi Arabia

Mathew Stewart[1*], Julien Louys[2], Huw S. Groucutt[3,4], Ian Candy[5], Richard Clark-Wilson[5], Paul S. Breeze[6], Nick A. Drake[4,6], Gilbert J. Price[7], Yahya S. A. Al-Mufarreh[8], Saleh A. Soubhi[8], Iyad S. Zalmout[8], Abdullah M. Alsharekh[9], Abdulaziz al Omari[10], Michael D. Petraglia[4]

[1] Palaeontology, Geobiology and Earth Archives Research Centre, School of Biological, Earth and Environmental Science, University of New South Wales, Sydney 2052, Australia.

[2] Australian Research Centre for Human Evolution (ARCHE), Environmental Futures Research Institute, Griffith University, Nathan, Queensland, Australia.

[3] Extreme Events Research Group, Max Planck Institute for Chemical Ecology, Hans-Knöll-Straße 8, 07745 Jena, Germany

[4] Department of Archaeology, Max Planck Institute for the Science of Human History, Kahlaische Strasse 10, 07745, Jena, Germany.

[5] Department of Geography, Royal Holloway, University of London, London, UK.

[6] Department of Geography, King's College London, London, UK.

[7] School of Earth and Environmental Sciences, University of Queensland, St Lucia 4072, QLD, Australia.

[8] Saudi Geological Survey, Sedimentary Rock and Palaeontology Department, Jeddah, Saudi Arabia.

[9] Department of Archaeology, King Saud University, Riyadh, Saudi Arabia.

[10] Saudi Commission for Tourism and National Heritage, Riyadh, Saudi Arabia.

Abstract

In recent years, the Arabian Peninsula has emerged as a key region for elucidating hominin and faunal evolution and dispersals between Africa and Eurasia. Central to this research is the middle Pleistocene site of Ti's al Ghadah (TAG) which has yielded a diverse and abundant fossil faunal assemblage and the earliest chronometrically dated evidence for hominins in this part of the world. Here, we present the first detailed taphonomic study of the large Unit 5 fossil assemblage from the site. We aim to assess which actor/s were responsible for the accumulation of the assemblage and evaluate evidence that might be consistent with the accumulation of fauna by hominins. We also describe, for the first time, fossils and lithic artefacts from stratigraphic horizons not previously considered, providing taphonomic insights into their accumulation. The taphonomic work shows that the Unit 5 faunal assemblage was accumulated by ambush predators, likely large felids and hominins, in a lake side environment, and that carcasses were subsequently scavenged by more durophagus carnivores such as hyenas and canids. Less can be reliably said regarding the newly described fossil assemblages given their poor preservation and significant wind abrasion, but large carnivores again appear to have played a role, and hominins probably played a role in the accumulation of at least one of these. This study provides the first detail insights into the interplay between hominins, carnivores, and herbivores in Arabia, and suggests that watering holes have been a focus on the Arabian landscape for resources since the middle Pleistocene.

Key words: Arabia; Butchery; Carnivore; Serial predation; Archaeology; Middle Palaeolithic.

*Corresponding author.

E-mail address: ms231@uowmail.edu.au

Present address: University of New South Wales, Sydney 2052, Australia.

1. Introduction

Over the past decade the Arabian Peninsula has seen a dramatic upturn in palaeontological, palaeoenvironmental, and archaeological research (e.g. Fleitmann et al., 2003, 2011; Parker, 2009; Armitage et al., 2011; Petraglia et al., 2011, 2012; Rosenberg et al., 2011, 2013; Delagnes et al., 2012; Groucutt and Petraglia, 2012; Scerri, 2012; Hilbert et al., 2014; Scerri et al., 2014b, 2015; Shipton et al., 2014; Breeze et al., 2015, 2016, 2017; Farrant et al., 2015; Groucutt et al., 2015a,b, 2016, 2018; Hoffmann et al., 2015; Jennings et al., 2015; Matter et al., 2015; Parton et al., 2015a, 2015b, 2018; Stimpson et al., 2015, 2016; Guagnin et al., 2018; Roberts et al., 2018). As a result, the significance of Arabia as a stage for African and Eurasian biotic exchanges throughout the Pleistocene and Holocene is increasingly apparent (Stewart et al., 2017), and it is now evident that hominins dispersed into Arabia by the middle Pleistocene (Groucutt and Petraglia, 2012; Jennings et al., 2015; Scerri et al., 2015; Roberts et al., 2018; Scerri et al., 2018). This is, however, unsurprising considering the Arabian Peninsula's geographical positioning at the crossroads of Africa and Eurasia, and the episodic increases in precipitation and water availability the peninsula experienced throughout the Pleistocene (Drake et al., 2013; Breeze et al., 2017; Roberts et al., 2018) that resulted in the establishment of palaeohydrological corridors that linked Arabia to northeast Africa and the Levant (Breeze et al., 2015, 2016; see also Vaks et al., 2007, 2010).

Corresponding influxes of diverse and novel taxa into the Arabian interior, as evidenced by the fossil record, provide further support for large-scale increases in water and grassland availability (McClure, 1984; Thomas et al., 1998; Stimpson et al., 2015, 2016; Groucutt et al., 2018). McClure (1984) was the first to report Pleistocene fossils from the Arabian Peninsula, following surveys of late Pleistocene and Holocene lacustrine deposits in the Empty Quarter (or Rub' al Khali) that yielded remains of *Bos*, *Bubalus*, *Gazella*, *Oyrx*, *Hippopotamus*, and possibly *Arabitragus jayakari*. Recent excavations at Shi'bat Dihya (SD1) in Yemen (Delagnes

et al., 2012) and Al Wusta in northern Saudi Arabia (Groucutt et al., 2018) recovered vertebrate fossil remains in direct stratigraphic association with Middle Palaeolithic artefacts. Significantly, the latter also produced a *H. sapiens* fossil phalanx dated to *c.* 85 ka, as well as fossil fauna consistent with well-watered and vegetated conditions, most notably *Hippopotamus* (Groucutt et al., 2018). This was further complemented by sedimentary and diatom analysis of the lake marls which indicated relatively shallow and stable freshwater conditions that likely attracted hominins, carnivores, and herbivores (Groucutt et al., 2018). Taphonomic assessment of the fossil assemblage found carnivore tooth marks and breakage patterns suggestive of at least partial accumulation by carnivores, however, the assemblage was too poorly preserved to provide more detailed insights (Groucutt et al., 2018).

Thomas et al. (1998) reported three fossil-bearing lacustrine deposits from the western Nefud Desert. Fossil fauna from these sites, notably alcelaphines, *Palaeoloxodon*, *Pelorovis*, and *Geochelone* sp. cf. *G sulcata*, were argued to reflect past savanna-like conditions in the region, which was further supported by isotopic analysis of fossil fauna teeth that demonstrated an abundance of C_4 grasses in the diets of herbivores (Thomas et al., 1998). Thomas et al. (1998) proposed an early Pleistocene age for the sites based on their interpretation of a mostly extinct fossil faunal assemblage, although more recent radiometric and optically stimulated luminescence (OSL) dating efforts have tied these sites to the pluvial intervals of the middle and late Pleistocene (Rosenberg et al., 2013; Stimpson et al., 2016). Of these three sites, Ti's al Ghadah (locality 2 of Thomas et al., 1998) yielded the largest, best preserved, and most diverse fossil assemblage (see also Stimpson et al., 2015, 2016). Fossils were recovered from a sandy horizon beneath a thick palaeolacustrine deposit and included a relative abundance of *Oyrx* fossils, as well as remains of Alcelaphinae, Camelidae, *Vulpes* sp., *Equus* sp., a large osteoglosiform fish, and provisionally identified remains of *Panthera gombaszoegensis* and *Palaeoloxodon recki*.

Stimpson et al. (2015, 2016) provided the first systematic study of Ti's al Ghadah which involved the excavation of six trenches spanning the southern half of the lacustrine exposure and targeting Unit 5 (see their Fig. 3). Combined Electron Spin Resonance (ESR) and U-series dating of fossil teeth, and OSL dating of the fossil-bearing and overlying lake sediments, placed the formation of Unit 5 between *c.* 500–300 ka, and more likely toward the older end of this range (Rosenberg et al., 2013; Stimpson et al., 2016). Excavations yielded abundant fossil material and increased the faunal diversity of the site. The presence of perennial water and expansive grasslands was further reinforced by the recovery of fossilised remains of fauna with strong affinities for water (*Anas, Tachybaptus*) and mesowear analysis of elephant molars (Stimpson et al., 2016). The presence of large carnivores (felids, hyenas, and canids) suggested that the western Nefud was host to a substantial prey biomass, and, by inference, a substantial biomass of vegetation (Stimpson et al., 2016). Direct fossil evidence for the presence of large predators (*Panthera* sp. cf. *P. gombaszoegensis*, cf. *Crocuta crocuta*) and scavengers (*Neophron percnopterus*, cf. varanids), coupled with carnivore tooth-marked bird, equid, and bovid skeletal remains, further suggested that the assemblage was at least in part the result of carnivore accumulation and feeding behaviours (Stimpson et al., 2016). Preliminary taphonomic analysis also found differences in taxonomic representation and preservation between the southern and northern part of the site, although possible processes controlling for these differences were not fully explored.

Cursory investigations of other parts of the basin have reported surface scatters of lithic artefacts and fossil material. Scerri et al. (2015) reported 76 Middle Palaeolithic artefacts from either side of the main palaeolake deposit (region shaded blue in Fig. 1), as well as fossils scattered across the basin. While it is not entirely clear how these relate to the stratigraphy and chronology of the site, given the available dates for the site and the broadly Middle Palaeolithic character of the lithics, they potentially represent the earliest Middle Palaeolithic assemblage

121 in Arabia (Scerri et al., 2015). Stimpson et al. (2016: 16) noted that ephemeral gullies had
122 "eroded fossils from the main lake ridge, re-depositing them unconformably downslope" and
123 reported that older and younger phases of lake formation were preserved within the basin,
124 although their precise stratigraphic positioning was not described.

125 Renewed investigations of the Unit 5 deposit recovered Middle Palaeolithic artefacts in
126 direct association with the Unit 5 fossils, as well as tentatively identified evidence for the
127 butchery of ungulate remains (Roberts et al., 2018). Significantly, these findings represent the
128 oldest chronometrically dated hominin presence in Arabia (*c.* 500–300 ka) and the second
129 Pleistocene site in Arabia demonstrating an unambiguous link between hominins and fossil
130 fauna (Roberts et al., 2018) – the other being the nearby late Pleistocene site of Al Wusta
131 (Groucutt et al., 2018). Stable carbon and oxygen isotope analysis of fossil herbivore teeth from
132 Unit 5 demonstrated productive grasslands and precipitation and humidity levels akin to
133 modern-day East African savannas (Roberts et al., 2018). Roberts et al. (2018) argued that this,
134 coupled with evidence for hominins at the site, demonstrated that middle Pleistocene hominin
135 dispersals into the Arabian interior required no major novel adaptations. Yet, a key line of
136 evidence for documenting the interactions between hominins, predators, prey, and the
137 environment within Arabia is missing – that is, detailed taphonomic investigations of the fossil
138 assemblages. Here, we present an important step towards addressing this issue by reporting a
139 detailed taphonomic analysis of the well-preserved chronometrically- and stratigraphically-
140 constrained Unit 5 fossil assemblage.

141 Taphonomic analyses are powerful tools for elucidating the role of biotic and abiotic
142 agents in the accumulation of fossil assemblages (Lyman, 1994). The early recognition that the
143 ways in which hominins and carnivores process carcasses is inextricably tied to feeding
144 behaviour, order of access, and inter- and intra-taxon competition led to a suite of controlled
145 actualistic and naturalistic studies that set out to identify how different bone modifiers may be

differentiated from the fossil record (e.g. Blumenschine, 1986, 1988; Marean and Spencer, 1991; Marean et al., 1992; Selvaggio, 1994, Capaldo, 1997, 1998). Such studies demonstrated that the types of prey animals and their ages (e.g. Stiner, 1990; Bunn and Pickering, 2010), skeletal part representation and fragmentation (e.g. Blumenschine, 1986, 1988; Marean and Spencer, 1991; Marean et al., 1992; Faith and Behrensmeyer, 2006; Faith et al., 2007), and the types of bone surface modifications, their location, and frequency (e.g. Blumenschine, 1986, 1988; Capaldo, 1997; Domínguez-Rodrigo, 1999) are reliable indicators of the accumulating agent or agents. For example, it has been repeatedly shown that the damage inflicted on long bone midshafts by hyenas varies greatly depending on whether hyenas have primary or secondary access to carcass parts (Blumenschine, 1988; Capaldo, 1997). Likewise, cut marked long bone midshafts are expected only if hominins had primary access to carcasses or obtained them with substantial scavengable flesh, as is sometimes the case following consumption by large felids (Pobiner, 2007).

This paper has five primary aims:

(1) We report the results of our geological study of the basin, allowing us to elucidate the relationship between the previously identified but unstudied stratigraphic units, log sections, and sample for diatom analysis in order to gain further insights into the nature of the lacustrine environments in the basin.

(2) We describe systematically collected fossils and lithic artefacts from stratigraphic horizons not considered previously, providing taphonomic insights into their accumulation. These include taxa identified from new deposits as well as those from recent excavations of Unit 5.

(3) We conduct inter-trench comparisons with newly collected data to investigate differences in taxonomic representation and preservation between the northern and southern part of the site and explore what this means for the site formation.

(4) By examining several taphonomic indications, we assess which actor or actors were primarily responsible for the accumulation of the Unit 5 fossil assemblage

(5) And lastly, we evaluate evidence, outside direct butchery marks, that might be consistent with accumulation of fauna by hominins.

2. Geographic and geological setting

The site of TAG is situated within an interdunal depression in the southwestern Nefud Desert, approximately 95 km southeast of the city of Tayma, Saudi Arabia (Fig. 1; 27.4330 N, 39.3725 E). The basin lies between two major NW-SE trending traverse barchanoid compound dunes, within which the dominant geomorphological feature is a large NW-SE trending palaeolake deposit that outcrops over 630 meters and rises to 6 m above the basin floor (Fig. 1). Renewed investigations at the site in 2017 extended the stratigraphic sequence to 10 meters below the modern-day surface of the main palaeolake and recognised three additional fossiliferous and artefact-bearing deposits (Figs. 1 and 2). Although the stratigraphy used in this study closely follows that of Stimpson et al (2015, 2016), our research suggests greater depth and complexity. The following summarises the sequence, and highlights modifications to the previously described stratigraphy.

We recorded a ~50 cm thick iron-rich lake marl deposit occurring at the base of the section (here referred to as Iron Lake; IL), that can be further subdivided into laminated (IL A) and massive (IL B) marls. While IL is clearly a distinct unit from the under- and overlying Unit 1 aeolian sands, it is referred to as "IL" and not "Unit 2" to maintain stratigraphic consistency between previous studies (i.e. Stimpson et al., 2016) and this one. The two lowermost fossiliferous levels occur directly beneath and atop the IL deposit. The most basal of these is a sandstone ridge (2611 m^2) situated between the main palaeolake deposit to the east and the large barchan dune to the west (here referred to as the Ti's al Ghadah Sandstone Ridge; TSR).

The ridge, which comprises sandstone capped by small *in situ* fragmentary deposits of IL A, declines westward and is eventually overlain by modern sands. Fossils were recovered from atop and eroding out of this ridge and in some instances fossils retained sandstone cemented to their surfaces, while some lithic artefacts were also recovered as surface finds. Small channels draining from the main palaeolake sequence have eroded and redeposited fossil material downward and westward so that mixing of distinct fossil deposits has occurred, as previously reported by Stimpson et al. (2016). Nevertheless, the fossils from these stratigraphic units appear to be easily distinguishable based on differences in preservation and appearance, such as the presence of cemented sandstone and lighter colour/patina for the TSR fossils.

The second fossiliferous and artefact-bearing level was located just north of TSR and situated stratigraphically above (here referred to as Ti's al Ghadah Iron Lake; TIL). The fossils were found atop the IL B marl (8151 m^2) and the similar sedimentary characteristics between IL A and IL B suggest that they may be laterally continuous with each other and part of the same deposit. Fossils were poorly preserved and share the colour characteristics of the marl suggesting that they are eroded from it. We hypothesize that the TSR and TIL fossils that sandwich the ferruginous marls (IL A and IL B) relate to the expansion and contraction of the lake – that is, the TSR fossils were deposited prior to the lake expanding, whereas the TIL fossils were deposited following the lakes contraction. The Unit 1 aeolian sands extend stratigraphically another 6.5 meters above the TIL deposit, indicating a period of increase aridity and dune mobility.

The greatest sedimentary complexity occurs in the top 2.5 meters of the sequence. The basal two meters are characterised by a succession of cross/horizontally-bedded, pebbly greenish sands that contain abundant root traces (Units 2–5). These are interpreted as reflecting deposition within more humid conditions in association with sheet/surface-wash processes at the margin of the lake basin. This is evidenced by the bedding structures and the presence of

pebble sized-clasts. The root traces indicate the presence of vegetation cover that episodically stabilised the land surface, while the greenish sands are interpreted as reflecting elevated groundwater levels and the existence of anoxic conditions. It is within the Unit 5 sands that the major fossil deposit was found, as reported by Thomas et al. (1998) and Stimpson et al. (2015, 2016).

The development of a more extensive lake body is indicated by Units 6–9 which record well-developed marl beds; however, the presence of gypsum crystals, sand beds, and tepee structures indicate that the lake underwent regular drying and desiccation. The stratigraphically youngest fossil bed lies on and within the uppermost section of Unit 9 (21322 m^2) which comprises a series of interbedded sands and gypsiferous marls incised with desiccation cracks that formed during the lake's final desiccation event (here referred to as Ti's al Ghadah Lake Surface; TLS). Progressively thicker palaeolake sediments moving southward suggest that the lake depocenter laid somewhere to the south of the current palaeolake exposure but has since been eroded. Fragmentary fossils and lithic artefacts were found widely scattered across the surface of the deposit. The greatest concentration occurred towards the southern end of the palaeolake exposure and *in situ* fossils were recovered around its north-western margins. The provenance of the majority of the TLS fossils is uncertain due to most being surface finds, although the few *in situ* fossils recovered from the marl strongly suggest the original depositional context was part of the uppermost unit, with similar states of preservation and appearance suggestive of a single provenance. Nevertheless, the possibility that some of these fossils originated in a discrete but eroded layer that was above the current capping unit cannot be discounted. We hypothesize that the Unit 5 and TLS fossil beds that sandwich the lacustrine marl (Units 6–9) are related to the expansion and contraction of a second younger lake.

PLACE FIGURE 1 AROUND HERE

PLACE FIGURE 2 AROUND HERE

4. Methods

4.1 Diatom analysis

Nine samples for diatom analysis were taken from the ILA, ILB, and Unit 6 diatomaceous marls at a 5 cm spacing. Different methods for diatom analyses were used to produce optimal results due to the low abundance and poor preservation of the diatoms. The standard methods (Renberg et al., 1990) include heating pre-weighed samples in 5ml of 30% hydrogen perioxide (H_2O_2) in test tubes at 90°C until the organic material had been digested, which may take up to two days. Once the tubes had cooled a few drops of 5% hydrochloric acid (HCl) were added to each test tube to remove any remaining carbonates prior to filling the tube with distilled water. The test tubes were settled overnight at 4°C before rinsing the next day. This process was repeated for four consecutive days to ensure samples were clean for slide preparation. A known volume of microspheres was added to the supernatant after the last rinse prior to adjust for the low and high concentrations of each slide (Battarbee and Kneen, 1982). Slides were air-dried at room temperature in a dust free environment for one to two days before mounting with Naphrax diatom mountant. A pilot study was undertaken to find an appropriate concentration and also an alternative method for diatom analysis in attempt to improve the low yield. Following earlier studies (Stoermer et al., 1995; Owen, 2010), the method using HCl was adapted by increasing the concentration of HCl from 10% to 30% and pre-soaking samples to increase the removal of carbonates and ensure cleaner slides which produced similar abundances to the standard methods confirming the low abundances and poor preservation of algae. Diatom taxa were plotted as percentage abundance and the resulting diatom diagrams zoned on the basis of the weighted average distribution of each taxon (Fig. S1 and S2). Both

TIL and Unit 6 deposits contained a relatively low abundance of diatoms and the resulting interpretations should be considered with caution.

4.2 Fossil recovery and identification

Excavations of the Unit 5 fossil-bearing layer by the Palaeodeserts Project and the Saudi Geological Survey (SGS) between 2013 and 2017 have produced 2001 fossil faunal remains that include birds, reptiles, and mammals (see Stimpson et al., 2015, 2016), as well as lithic artefacts (Roberts et al., 2018). All fossils recovered from Unit 5 have been examined, although not all were included in the present analysis. Fossils recovered during unscreened excavations by the SGS of the Elephant Quarry (n=329), a trench located at the southern part of the palaeolake deposit, were excluded from the main taphonomic analysis but are nonetheless discussed in some detail where we believe this to be informative. The remaining fossil material (n=1672) was recovered during excavation of six trenches by the Palaeodeserts Project between 2013 and 2014. All excavated sediment was dry screened using 2 mm mesh sieves, and the locations of diagnostic specimens >5 mm in maximum dimension were recorded by total station (Stimpson et al., 2016). Twenty-eight specimens were excluded from the final dataset due to insufficient data collection information and we consider the remaining fossil assemblage to be the Number of Recovered Specimens (NRSP=1644) for analytical purposes. Taphonomic winnowing of unidentifiable fragments <20 mm in maximum dimension (n=1042) further reduced the assemblage that can be analysed, and we refer the remaining fossils to the Number of Identified Specimens (NISP=602). No winnowing based on cortical preservation was conducted, but we note that overall the fossils are well-preserved and exhibited minimal abrasion and cortical exfoliation. A small portion of identified fossils (n=60) were recovered from Unit 5 but no further information regarding which of the trenches they came from was recorded. These fossils were included in the analysis but were excluded from inter-trench

comparisons. Thomas et al. (1998) also collected fossils from what is believed to be Unit 5, and although the material they collected was examined by one of us (MS), where each fossil originated from of the three locations reported in their paper is not possible to discern, and, therefore, we have not included their material in the present study.

Pedestrian line surveys of the TSR, TIL, and TLS palaeolake deposits were conducted during the 2017 field season. Surveys were conducted by eight to ten people walking together in a straight line and separated by no more than three meters. The entire exposure of each palaeolake deposit was examined and all fossils collected, and their positions recorded by differential global positioning system (DGPS). When fossils were discovered the group halted while fossil location was recorded, specimen numbered, and bagged. Any fossils found eroding out of the palaeolake sediments were carefully removed. The NRSP for the TSR, TIL, and TSR assemblages are 848, 14, and 801, respectively. Taphonomic winnowing of small and unidentifiable fragments produced an analytical assemblage (NISP) of 622, 5, and 441, respectively. Fossils deemed to have been redeposited downslope from atop the main palaeolake deposit (n=212) were excluded from the analysis.

Fossil identification and analysis was conducted at the Australian National University (ANU) and the University of New South Wales (UNSW), Australia. Each fossil specimen was identified to the lowest taxonomic level possible and facilitated by osteological collections housed at the abovementioned institutes and the Smithsonian National Museum of Natural History (NMNH), USA. Specimen morphometric data (length, breadth) was obtained using digital callipers and additional morphometric measures taken following von den Driesch (1976). The key taphonomic principals considered in this study (skeletal part representation, animal size classes, bone fragmentation, bone surface modifications, and mortality profiles) are described below.

4.3 Quantitative units

Results were described using four standard quantitative units: NRSP, NISP, Minimum Number of Elements (MNE); and Minimum Number of Individuals (MNI) (see Lyman, 1994 for a detailed discussion on these quantitative units). MNE was calculated as the minimum number of skeletal units – whole elements (e.g. humerus) or part thereof (e.g. distal humerus) – needed to account for all specimens of a given skeletal unit without taking into consideration the age or side of the animal (Bunn and Kroll, 1986). MNI values were determined similarly to MNE but taking into consideration the age (based on tooth wear, epiphyseal fusion, and bone texture in the case of neonates) and side (for bilaterally paired elements) of the animal. Quantitative units were also normalised (%NISP, %MNE) by dividing all values by the greatest value and multiplying by one hundred (Binford, 1984) to aid in inter-site and inter-study comparisons of skeletal part representation.

4.4 Animal size class

Specimens were assigned a size category corresponding to the five size-classes described in Bunn (1982), where small, medium, and large denote size classes I-II (< 100 kg; e.g. foxes, gazelle), III-IV (100 kg – 340 kg; e.g. wild asses, oryx), and V-VI (> 340 kg; e.g. hippos, elephant), respectively. The small animal size class includes microfauna (reptiles, birds, rodents), carnivores, and small ungulates, and these groups are often considered separately throughout the present study to highlight differences in the treatment and preservation of these groups.

4.5 Bone fragmentation, breakage, and completeness

The analysis of post-depositional fragmentation can provide important insights into the timing and agent of the accumulation of fossil assemblages and represents an important initial

step in any taphonomic analysis as skeletal part representation and bone surface modification frequencies are likely to be impacted by the degree of fragmentation. The most basic of these is specimen maximum dimension (or length) which is reported in 10 mm bins up to 100 mm. Two fragmentation ratios based on fossil identifiability are also reported: NRSP/NISP and NISP/MNE for investigating inter-trench and size-biased differences in fragmentation, respectively (see Cannon, 2003). The former is less sensitive to increasing fragmentation than other fragmentation indices, but as it is based on NRSP it cannot be used to investigate taxon- or size-specific differences in fragmentation (Cannon, 2003); for this, we use the second ratio.

Long bone circumference completeness (%) was recorded using the three categories described in Bunn (1982): less than half (Type 1), more than half but not complete (Type 2), and complete (Type 3). During carcass processing and consumption, hominins and large bone-crushing carnivores systematically break open long bones to exploit marrow and as a result tend to generate assemblages dominated by Type 1 shafts (Bunn, 1982; Marean and Spencer, 1991; Marean et al., 2004). On the other hand, less bone-destructive carnivores such as canids and felids typically produce assemblages that comprise more Type 2 and Type 3 shafts (Sala et al., 2014; Arriaza et al., 2016). Consequently, the relative abundance of fragmented and complete long bone shafts provides a valuable means for investigating the role of hominins and carnivores in the accumulation of fossil assemblages.

As a final measure of fragmentation, we recorded long bone fracture patterns as green or dry based on the criteria described by Villa and Mahieu (1991). Bones broken while green (or 'fresh') typically exhibit obtuse or acute fracture angles, a curved outline, and smooth fracture edge, whereas bones broken while in a dry state produce transverse fractures with jagged and stepped edges (Villa and Mahieu, 1991). Bones were recorded as intermediate if they exhibited traits typical of both green and dry broken bones.

362 *4.6 Skeletal part representation*

363 Skeletal part representation can provide important insights into the differential
364 treatment and transport of bones by hominins, carnivores, and abiotic processes such as fluvial
365 transport and post-burial destruction. The relative proportions of each skeletal part were
366 examined according to NISP and MNE. Moreover, we considered the relative proportions of
367 skeletal elements according to body section: skull (cranium, mandible), axial (vertebrae),
368 forelimb (scapula, humerus, radius, ulna), hindlimb (pelvis, femur, tibia, patella), distal limb
369 (carpals, tarsals, metapodials), and feet (phalanges, sesamoids).

370 Post-depositional survival of skeletal elements is in large part mediated by the physical
371 properties of bone – most notably density – which differ significantly from one skeletal element
372 to another (Lyman, 1984; Lam et al., 1998, 1999). A common method for assessing the role of
373 post-depositional processes in mediating skeletal part representation is to examine the
374 relationship between skeletal part representation and bone mineral density (e.g. Lyman, 1984,
375 Lam et al., 1998, 1999; Faith and Behrensmeyer, 2006; Faith et al., 2007). For small- and
376 medium-sized ungulates we used bone mineral density values calculated from goat (Lam et al.,
377 1998) and wildebeest (Lam et al., 1999) bones, respectively, and corrected for shape and
378 internal cavities when available (BMD_2).

379 Interpretations of skeletal part representation are complicated by the fact that most
380 high-density elements are low in economic utility, and most low-density elements high in
381 economic utility (Lyman, 1994). Consequently, skeletal part profiles suffer from equifinality
382 in that various abiotic (e.g. hydraulic winnowing, post-burial destruction) and biotic (e.g.
383 carnivore processing, trampling, hominin transport) processes may generate fossil assemblages
384 that comprise a similar set of skeletal elements. This issue of equifinality may, however, be
385 overcome by considering the economic utility of skeletal elements present in an assemblage,

as well as the frequency and location of bone surface modifications which Domínguez-Rodrigo et al. (2007b) refer to as the "physical attribute" taphonomic approach (see also Bar-Oz and Munro, 2004 and references therein). Given that hominins are evidenced at the site by lithic artefacts and probably butchered bones of medium-sized ungulates (Roberts et al., 2018), it is important to consider the possibility that hominins shaped the Unit 5 fossil assemblage by transporting skeletal elements to or from the site. To do so, we compared the skeletal part survivorship to Metcalfe and Jones' (1988) Standardized Food Utility Index (SFUI) for domestic sheep bones. Faith and Gordon (2007) recommend that "low-survival" elements be removed from such analyses as these are readily destroyed by various taphonomic processes (e.g. weathering, carnivore processing, trampling) and are therefore not well-suited for addressing questions regarding hominin butchery and transport decisions in assemblages variously affected by destructive processes. Accordingly, we compared the skeletal part survivorship and SFUI using low- and high-survival elements and high-survival elements only (i.e. crania, mandible, humerus, radius, metacarpal, femur, tibia, and metatarsal).

Considering the lacustrine setting within which the fossils were deposited (Rosenberg et al., 2013; Stimpson et al., 2015, 2016), it is worth investigating the possibility that the assemblages have undergone hydraulic winnowing. Bones have different transport potentials in water, governed by their shape and density, and, as a result, assemblages significantly influenced by hydraulic winnowing will be overrepresented by elements with either high (transported component) or low (lag component) transport potentials (Voorhies, 1969; Behrensmeyer, 1975; Dechant Boaz and Behrensmeyer, 1976; Fernández-Jalvo and Andrews, 2003). Fossils were placed into transport groups following Voorhies (1969): Group I, bones that float and are highly susceptible to transport (e.g. vertebrae); Group II, bones that are less susceptible to transport and drag as oppose to float (e.g. limb bones); and Group III, the least susceptible to transport (e.g. mandible). As an additional measure for hydraulic influence we

411 calculated the tooth to vertebrae ratio, with values between 0.44–1.5 indicating limited or no
412 hydraulic influence, and values of 3.12–3.48 indicating strong hydraulic influence
413 (Behrensmeyer, 1975).

414 *4.7 Bone surface modifications*

415 Each specimen was examined for surface modifications by eye and hand-lens (10-20x)
416 and under different exposures of light to assist in the identification of fine-scale modifications.
417 Closer inspection of selected bone surface modifications was carried out using a binocular
418 microscope (up to 80x) and Scanning Electron Microscopy (SEM; Hitachi S-3400N) in
419 variable-pressure mode (VP-SEM) to capture backscatter (BSE) images of the sample surfaces
420 with specimens mounted on SEM stubs using Leit-C-Plast™ carbon-based removable
421 adhesive. Fossils were inspected for cut marks, hammerstone percussion marks, carnivore and
422 rodent gnawing, trampling marks, abrasion, weathering, root etching, and staining, and the
423 anatomical location of each modification recorded.

424 Cut marks were defined as linear V-shaped grooves often with accompanying shoulder
425 effect, shoulder flaking, and internal microstriations: shoulder effect was defined as shallow
426 striae associated with and running parallel to, but not more than 0.2 mm from, the main groove;
427 shoulder flaking refers to flaking dents that occur along all or part of the edge of the main
428 groove; and internal microstriations were defined as shallow striae within the main groove and
429 visible at 40x magnification (Olsen and Shipman, 1988; Fisher, 1995; Domínguez-Rodrigo et
430 al., 2009). Trampling marks were differentiated from cut marks in exhibiting a sinuous
431 trajectory, diverse and intersecting striations, and no or irregular internal microstriations (Olsen
432 and Shipman, 1988; Domínguez-Rodrigo et al., 2009). Hammerstone percussion marks refer
433 to pits, grooves, notches, and isolated patches of microstriations (Blumenschine, 1995).
434 Percussion pits are described as shallow U-shaped indentations. These may macroscopically

435 resemble carnivore tooth pits but differ microscopically by the presence of microstriations
436 occurring within or emanating from the pit as a result hammerstone slippage following contact
437 with the cortical surface (Blumenschine and Selvaggio, 1988). Moreover, percussion pits
438 typically lack the crushing of the cortical surface commonly observed in carnivore tooth pits
439 (Blumenschine, 1995). Percussion notches were defined as broad arcuate breaks in the edge of
440 long bone midshafts with corresponding conchoidal medullary flake scars, whereas those
441 produced by carnivores are typically more circular and narrower (Capaldo and Blumenschine,
442 1994). Carnivore tooth marks were classified into pits, scores, furrows, and punctures
443 following Binford (1981): pits were defined as shallow U-shaped impressions often with
444 crushing of the cortical bone; scores refer to shallow U-shaped longitudinal grooves in the
445 cortical bone; punctures, which include notches, refer to complete perforations of compact
446 bone; and furrows defined as the removal/gouging of cancellous bone. Carnivore tooth pit and
447 puncture mark maximum length and breadth measures were taken following Domínguez-
448 Rodrigo and Piqueras (2003) and were compared to tooth mark dimensions from the literature
449 (e.g. Domínguez-Rodrigo and Piqueras, 2003; Delaney-Rivera et al., 2009; Sala et al., 2013).
450 The frequency, location, and qualities of butchery and tooth marks can provided unique insights
451 into the role of hominins and carnivores in the accumulation of fossil assemblages and we
452 compare the data from the present study to landscape and actualistic studies modelling hominin
453 and carnivore feeding behaviours (e.g. Blumenschine, 1986, 1988, 1995; Marean and Spencer,
454 1991; Marean et al., 1992; Capaldo, 1997, 1998; Faith and Behrensmeyer, 2006; Faith et al.,
455 2007; Gidna et al., 2014; Sala et al., 2014; Organista et al., 2016).

456 Rodent gnawing marks were described as parallel chisel-like groves with relatively flat
457 bases (Brain, 1981; Maguire et al., 1980). Root marks, which are generated by the dissolution
458 of bone tissue by chemicals produced directly or indirectly by plant roots, are defined as U-
459 shaped branched grooves often occurring in dense concentrations (Fernández-Jalvo and

460 Andrews, 2016). Each specimen was assigned a weathering stage ranging from zero to five
461 following Behrensmeyer (1978) where stages zero and five represent un-weathered and
462 extensively weathered specimens, respectively.

463 *4.8 Mortality profile analysis*

464 Mortality profiles, also known as age-frequency distributions, are powerful tools for
465 inferring hominin and carnivore prey selectively and procurement strategies (Bunn and
466 Pickering, 2010). These are often grouped into three main mortality profile models useful for
467 inferring the mode of death of prey populations: catastrophic/living structure, attritional/U-
468 shaped, and prime-age dominated (Stiner, 1990; Bunn and Pickering, 2010; see also Discamps
469 and Costamagno, 2015 and references therein). Catastrophic/living structure mortality profiles
470 resemble stable living populations (that is, there are fewer individuals in successive age classes)
471 indicating that the mode of death was non-biased with respect to age or physical condition and
472 are typically considered illustrative of non-selective ambush hunting (e.g. lion predation) or
473 catastrophic mass death events (e.g. mass kills, flooding, fire, disease). Attritional/U-shaped
474 mortality profiles comprise more weaker juvenile and old individuals that are typically targeted
475 by social cursorial predators (e.g. cheetahs, African wild dogs), although such profiles may
476 also be generated by disease and malnutrition largely affecting weaker individuals (Delgiudice
477 et al., 2006). In contrast, prime-aged dominated mortality profiles comprise mostly the fittest
478 individuals in a population and are often attributed to selective predation by hominins (Stiner,
479 1990), but, in some cases, may also arise from natural, non-anthropogenic processes (e.g.
480 Wolverton, 2001; Kahlke and Gaudzinski, 2005; Price, 2008).

481 Mortality profiles were constructed for medium-sized bovids using mandibular tooth-
482 wear stages and specimens placed into one of five age groups following Bunn and Pickering
483 (2010): (1) young juvenile, light to moderately worn deciduous molars and erupting first and

second molars; (2) subadult juveniles, moderate to heavily worn or shed deciduous molars and erupting or erupted permanent premolars and molar; (3) early prime, complete permanent dentition with light to moderate wear and without loss of molar infundibulum; (4) late prime, greater wear and no loss of M_1 mesial infundibulum; (5) old, heavy occlusal wear and loss of mesial and distal molar infundibulum. Taphonomic processes (e.g. carnivore feeding, weathering) are known to disproportionately affect young juvenile remains (Behrensmeyer, 1978; Munson, 2000l Munson and Gerniewicz, 2003) and, as such, mortality profile analyses excluding young juvenile remains were also conducted (following Bunn and Pickering, 2010). Mortality profiles were analysed and graphed using the updated modified triangular graph program of Weaver et al. (2011). This program uses likelihood statistics to generate 95% density contours allowing for statistical comparisons between mortality profiles: if the density contours of two samples do not intersect, they are considered to differ at a level of statistical significance. Mortality profiles were also compared using Chi-squared test, or Fisher's exact test when expected values fell below five. We compared the Unit 5 data to mortality profiles of carnivore hunted medium-sized ungulates, as well as ethnographic (Hadza, Kua) and archaeological mortality data. Despite some within-carnivore species and within-predation strategy (ambush vs. cursorial) differences in mortality data – for example, lions in the Kafue National Park were found to take more prime-aged individual than lions in the Serengeti – when plotted in ternary diagrams, the density contours of individual carnivore species and hunting strategies tend to overlap (Oliver et al., 2019). Therefore, we follow Oliver et al. (2019) in pooling species mortality profile data, as well as ambush (lion, leopard) and cursorial (hyena, wild dog) predators.

4.9 Lithic analysis

Lithics were classified and recorded according to the methods outlined previously by Groucutt et al. (2015a,b, 2018) and Scerri et al. (2014a, b). This analysis describes the typological and technological features of the assemblages to allow basic comparison to other assemblages. We recorded raw material type, typological category and basic metrics (length, width and thickness) using digital callipers. These characteristics offer an overview of the lithic assemblages, providing both behavioural and taphonomic information for the site.

4.10 Statistical analysis

Chi-squared tests were used to investigate the likelihood of independence between two ordinal or nominal variables when expected counts were greater than or equal to five. When expected counts were below five, we used a Fisher's Exact Test instead. Spearman's Rank Order (r_s) and Pearson's Correlation Coefficients (r) were used to measure the strength of the linear association between two variables. Statistical analyses were carried out in PAST (Hammer et al., 2001) and graphics generated using the ggplot2 package (Wickham, 2016) in RStudio (RStudio Team, 2015).

5. Results

5.1 Diatom analysis

Diatom assemblages were recovered from the ferruginous marls (IL A and IL B) and Unit 6. Although the abundance of diatoms was low (yielding about half what is considered sufficient for a statistically valid dataset) they indicate the existence of freshwater, but typically slightly saline/brackish water bodies at this time (Fig. S1 and S2). In IL B, the dominance of *Staurosirella lapponica*, in samples with the highest number of identifiable valves, implies alkaline lake conditions, whereas the change from a planktonic assemblage towards the base

(*Lindavia comensis*) to a benthic dominate assemblage towards the top (*S. lapponica*) implies the water body was shallowing. The brackish nature of this water body is indicated by the presence of a number of salinity tolerant species: *Denticula kuetzingii*, *Navicula cincta*, and *Nitzschia sigma*. In Unit 6, the diatoms suggest a neutral/alkaline lake but less alkaline than TIL. *Aulacoseira crassipunctata*, for example, prefers freshwater of pH of ~5–6, whereas *S. pinnata* var. *intercedens* prefers pH of ~6.9–8.2. Unit 6 also appears to be less saline than the ferruginous marls as *N. sigma* is the only brackish tolerant species in the assemblage.

5.2 Systematic Palaeontology

Below we build on the taxonomic identifications of Thomas et al. (1998) and Stimpson et al. (2015, 2016) by describing novel taxa that were encountered during the taphonomic assessment of the Unit 5 fossil deposit (specimen catalogue prefixes: TAG, SGS), as well as identifiable material from the newly investigated deposits. Poor preservation of the TIL fossils prohibited confident taxonomic identification of any of the specimens, but we note that some clearly belong to a very large animal, probably an elephant or hippo. For a complete taxonomic list, we refer the reader to Table S1.

Class **REPTILIA** Laurenti, 1768

Order **SQUAMATA** Oppel, 1811

Renewed investigation of the Unit 5 fossil deposit recovered vertebrae belonging to at least two, and possibly three, species of Squamata. Osteological nomenclature and description of reptiles follows Hoffstetter and Gasc (1969) and Malnate (1972).

Squamata gen. et sp. indet. 1

A small sacrum (TAG14/9346, Trench 6) consists of two fused vertebrae, with slender pleurapophyses, and foramen sacrale. There appears to be no bifurcation of the pleurapophysis

of the second vertebrae and a ventral foramen is absent, features which occur in Gekkonidae, Agamidae, and a few Iguanidae, but are not ubiquitous among all species of these families.

Squamata gen. et sp. indet. 2

A vertebra (TAG14/706, Trench 4) with procoelous centra, wide anteriorly positioned transverse processes, and lack of fracture plane, indicating one of the anterior caudal vertebrae. Lack of paired haemapophyses and a strong ventral sagittal ridge suggest this specimen is neither a varanid or *Uromastyx* sp. (Holmes et al., 2010).

Superfamily **COLUBROIDEA** Oppel, 1811

Colubroidea gen. et sp. indet.

A vertebra (TAG14/710, Trench 4) with a spheroidal joint articulation of the centrum is clearly that of a snake. The presence of a hypapophysis and pronounced neural spine preclude burrowing snakes (e.g. Uropeltidae, Leptotyphlopidae and Typhlopidae) and indicates one of the precaudal vertebra. An anterior keel leading from the hypapophysis is present but does not reach the cotyle. An anteroventrally directed parapophysial process is present, a feature that occurs mainly in the colubroid snakes, and we assign the Unit 5 specimen to the Colubroidea superfamily accordingly.

Class **MAMMALIA** Linnaeus, 1758

Order **LAGOMORPHA** Brandt, 1855

Family **LEPORIDAE** Fischer de Waldheim, 1817

Leporidae gen. et sp. indet.

Left mandible (TAG14/9373, Trench 1) with M_1 and M_2 in place. Both molars are similar in form, although the M_2 is slightly simpler in its overall outline. Each molar displays deep infolding and the posterior lobe is significantly lower than the anterior. Molar morphology

differs little among genera of this family, and *Oryctolagus*, *Lepus*, and *Sylvilagus* all overlap in their cheek teeth dimensions, and, as such, we assign this specimen to family level only.

Order **RODENTIA** Bowdich, 1821

Rodentia gen. et sp. indet.

A single incisor (TAG14/709, Trench 4) with enamel restricted to the buccal surface is clearly that of a rodent, however it is not possible to identify this specimen further.

Order **PROBOSCIDEA** Illiger, 1811

Family **ELEPHANTIDAE** Linnaeus, 1758

Elephantidae sp.

Various tooth enamel fragments (TLS/75, 5149, 5150) recovered from TLS are consistent with elephantids, but the fragments are small and poorly preserved and little more can be said regarding their taxonomy.

Order **PERRISODACTYLA** Owen, 1848

Family **EQUIDAE** Gray, 1821

Equidae gen. et sp. indet.

An equid metapodial fragment and single incisor were recovered from TSR and TIL, respectively, however these are poorly preserved and provide no further taxonomic insight.

Order **ARTIODACTYLA** Owen, 1848

Family **BOVIDAE** Gray, 1821

Subfamily **ALCELAPHINAE** Brooke, 1876

Alcelaphinae gen. et sp. indet.

596 Thomas et al. (1998, p. 149) reported "a few isolated lower and upper molars"
597 belonging to an alcelaphine from Unit 5, as well as the nearby late Pleistocene site of Khall
598 Amayshan, but provided no details regarding their appearance or size. Here we report two
599 additional specimens that we refer to Alcelaphinae: an isolated M^2 (SGS-NEFUD-57) and right
600 maxilla with M^1, M^2, and M^3 in place (SGS-NEFUD-225; Roberts et al., 2018, Fig. S3). Molars
601 are large and most consistent in size with the living wildebeest: *Connochaetes gnou* and *C.*
602 *taurinus* (Fig. S3). However, they differ from those of comparative specimens of wildebeest in
603 having simpler infundibula, and most notably so in the second molar. In this regard they more
604 closely resemble the teeth of *Alcelaphus* and the extinct *Rusingoryx* but differ from the latter
605 in having a more complex occlusal pattern and pronounced styles and ribs (see Faith et al.,
606 2011). Given the limited number of specimens and difficulties in distinguishing between like-
607 sized alcelaphines, we follow Thomas et al. (1998) in referring the specimens described here
608 to Alcelaphinae.

609 Subfamily **HIPPOTRAGINAE** Brooke, 1876

610 Genus **ORYX** de Blainville, 1816

611 *Oryx* sp.

612 Two left mandibles (TSR/9007, 9017) are referred to *Oryx* sp. (Fig. S4). Teeth have a
613 simple occlusal outline, ectostylids on the M_1 and M_2, and simple U-shaped infundibulum that
614 become progressively flatter towards the M_3. Second and third molars exhibit pronounced
615 parastylids and goat-folds, features which are often present in the desert-adapted *O. dammah*
616 but that are typically more subtle in *O. leucoryx*, *O. beisa*, *O. gazella*, and material from Unit
617 5 (cf. Stimpson et al., 2016, Fig. 12D). The TSR/9007 specimen is notably large and the length
618 of its M_2 (28.5 mm) and estimated length of its M_3 (38.4 mm) exceeds those of the living
619 species, as well as material from Unit 5 (Fig. S5). Thomas et al. (1998) and Stimpson et al.
620 (2016) suggested, based on tooth and palatine morphology, horn core divergence, and body

size estimates derived from long bones, that the *Oryx* present in the Unit 5 assemblage belonged to a large-bodied extinct form of the Arabian endemic *O. leucoryx*. Given the differences in morphology and large size of the TSR/9007 specimen, it seems reasonable to suggest that at least one other, even older species of *Oryx* may have inhabited the Arabian Peninsula and is represented in the TSR assemblage.

Subfamily **ANTILOPINAE** Gray, 1821

Antilopinae gen. et sp. indet.

A small, well-preserved bovid sacrum (SGS-NEFUD-55, Elephant Quarry) with a greatest length and breadth measuring 83.2 mm and 61.8 mm, respectively. *Oryx* can be discounted based on size alone, which in living species have greatest breadths ranging from 95–153 mm (*n*=36; data from Peters et al., 1997). Its size is more consistent with smaller antilopines, and the greatest breadth taken from a single comparative *Gazelle gazella* specimen near matched the specimen presented here (61.7mm, data taken from ref. specimen 100, A. Garrad's personal collection, UCL Institute of Archaeology). A small fragmented bovid proximal metacarpal (TSR/885) with an estimated proximal breadth of ~16–18 mm is also probably that of an antilopine and is also consistent in size with *G. gazella* (18.5–22.8 mm, *n*=25, data from Horwitz et al., 1990). Given the limited material, we attribute both specimens to the Antilopinae subfamily.

5.3 Taxonomic representation

Only a few additional taxa were recognised during the present study: a leporid, rodent, and at least two squamates (see Table S1 for complete taxonomic list). The Unit 5 assemblage has a high taxonomic diversity compared to other Pleistocene sites in the Arabian Peninsula with 15 orders and 19 families. The second most diverse fossil assemblage, for example, is the nearby late Pleistocene site of Al Wusta with 5 orders and 5 families.

The abundance of animals according to NISP, %NISP, and MNI is provided in Table 1 and displayed graphically in Figure 3. Medium-sized bovids are the dominant taxon in the Unit 5 deposit (39.2% of NISP), followed by birds (5.1% of NISP), carnivores (3.3% of NISP), small bovids (2.9% of NISP), elephants (2.8% of NISP), reptiles (2.1% of NISP), equids (1.1% of NISP), rodents and leporids (0.5% of NISP), camelids (0.2% of NISP), and indeterminate mammals of varying sizes (42.8% of NISP). Taxa were similarly represented when substituting NISP for MNE and a comparison of the two measures found them to be statistically indistinguishable ($\chi^2 = 1.38$, $p = 0.848$). *Oryx* is ten times more abundant than alcelaphines (based on MNI values from the Unit 5 and Elephant Quarry assemblages) and we follow earlier studies (Thomas et al., 1998; Stimpson et al., 2016) in suggesting that the bulk of the medium-sized bovid post-crania is attributable to an unidentified and probably undescribed species of *Oyrx*.

There are clear and statistically significant differences in taxonomic representation between the southern and northern trenches ($\chi^2 = 28.94$, $p < 0.001$). A trench-by-trench breakdown (Fig. 3) found that small animals are more common across all three of the southern trenches: rodents, reptiles, and birds are particularly abundant in trenches 2 and 4, whereas carnivores are best represented in trench 1. Equids and elephants are almost exclusively known from the southern trenches and are notably abundant in the Elephant Quarry fossil collection (equid NISP=13, elephant NISP=114). By contrast, the northern trenches are far less taxonomically rich and are overwhelmingly dominated by medium-sized ungulates, and more specifically bovids.

PLACE FIGURE 3 AROUND HERE

5.4 Taphonomic analysis

5.4.1 Bone fragmentation, breakage, and completeness

The results of the quantitative analysis of the bone surface modifications and fracture patterns are provided in Tables 2 and 3. The Unit 5 assemblage appears moderately fragmented with just under two thirds (61.9% of NRSP) comprising fragments less than 20 mm in maximum length (Fig. 4). This contrasts to highly fragmented fossil assemblage in which almost all fossils are small unidentifiable fragments (e.g. Clark, 2019). The Elephant Quarry assemblage displays an inverse pattern of specimen size distribution, although this is unsurprising given the lack of screening of this section of the site. Specimens greater than 20 mm in maximum length were more-or-less evenly represented in the Unit 5 assemblage. Large animal fossils less than 100 mm in length were rare, and, as such, it appears that their remains have undergone minimal post-depositional destruction. This is further supported by the recovery of complete fragile skeletal elements (ribs, vertebrae) and the discovery of fossils in semi-articulated positions in the Elephant Quarry. Medium-sized ungulates, too, appear to have undergone only moderate post-depositional destruction as evidenced by one third of their skeletal remains exceeding 100 mm in length. The recovery of many complete fragile bird and reptile remains also attests to the limited post-depositional destruction of the Unit 5 fossil assemblage. Fossils from the northern trenches are slightly less fragmented than those from the southern trenches but the distributions of specimen size are more-or-less alike: specimens less than 20 mm in maximum length make up 68% and 55% of the NRSP in the southern and northern trenches, respectively, while specimens of other length categories make up only a small portion each and are similarly represented.

PLACE FIGURE 4 AROUND HERE

690 Based on the NRSP/NISP ratio, the northern trenches (NRSP/NISP=2.1) are roughly
691 one third less fragmented than the southern (NRSP/NISP=2.9) trenches. Again, this difference
692 is largely driven by Trench 5 which comprises of entirely identifiable elements
693 (NRSP/NISP=1.0). There is little difference in fragmentation across animal size-classes, but
694 carnivores (NISP/MNE=1.1) are the least fragmented taxa, as would be expected in an
695 assemblage influenced by carnivore processing. As a final means of comparison, we compared
696 medium-sized ungulate fragmentation between the northern and southern trenches on the basis
697 that they are the most abundant and ubiquitous taxa represented in the Unit 5 deposit and should
698 therefore provide the best measure of inter-trench differences in fragmentation. Consistent with
699 the results presented above, medium-sized ungulates are less fragmented in the northern
700 (NISP/MNE=1.2) than southern (NISP/MNE=1.5) part of the site (Table S2).

701 The shaft ratio (Type 2 + Type 3:Type 1) for small- and medium-sized animals equals
702 5.0 and 1.76, respectively. Experimental scenarios modelling hominin and hyena feeding
703 behaviours found that the shaft ratio typically ranged between 0.13–0.44 (Marean et al., 2004;
704 Pickering and Egeland, 2006). Therefore, it appears that if hominins and hyenas modified the
705 Unit 5 assemblage, they did so only marginally. These ratios are, however, more consistent
706 with processing by other less bone destructive carnivores such as lions and wolves (Sala et al.,
707 2014; Arriaza et al., 2016). Indeed, a comparison of medium-sized ungulate carcasses
708 processed by wild and captive wolves and the Unit 5 assemblage found no significant
709 difference in shaft circumference completeness (Table 5). In contrast, the Elephant Quarry
710 assemblage shaft ratio (0.52) is more consistent with assemblages processed by hominins and
711 hyenas. An inter-trench comparison found no differences in shaft circumference completeness
712 between the northern and southern trenches across all taxa and size classes ($\chi^2 = 2.54$, $p =$
713 0.281) and for medium-sized ungulates only ($\chi^2 = 1.50$, $p = 0.472$). A statistically significant
714 difference was found, however, when comparing the shaft circumference completeness of

715 small- and medium-sized animals (χ^2 = 6.44, p = 0.040) indicating lesser fragmentation of the
716 former.

717 Long bone fracture patterns were considered as a final measure of post-depositional
718 fragmentation. Eighty-eight long bone were assessed based on their fracture angles, outline,
719 and edge characteristics. Of these, fragments displaying characteristics consistent with green
720 fracturing (*n*=43) were more common than those consistent with dry fracturing (*n*=34), while
721 a small portion was found to exhibit intermediate characteristics (*n*=11). Long bone fracturing,
722 therefore, occurred at various stages in the post-depositional history of the Unit 5 fossil
723 assemblage. No statistically significant difference was found when comparing the Unit 5 and
724 Elephant Quarry fracture patterns (χ^2 = 1.53, p = 0.216). Green fracturing can in part be
725 attributed to carnivore processing, as evidence by green fractured bones bearing large carnivore
726 tooth marks and notches (*n*=7), while dry fracturing is likely the combined result of weathering
727 and post-burial destruction. No difference in green and dry fractured bone was found between
728 small- and medium-sized animals (Fisher's Exact Test, p = 1.0). Green fractured bone of
729 medium-sized animals was more common in the southern than northern part of the site,
730 although this difference was found to be insignificant (χ^2 = 3.35, p = 0.067).

731 *5.4.2 Skeletal part representation*

732 Almost all elements of the vertebrate skeleton are represented in the Unit 5 assemblage
733 and a complete skeletal inventory is provided in Table 4. Elements of the crania, appendicular,
734 and forelimb are most abundant in term of NISP, but the former and the latter are greatly
735 reduced in terms of MNE (Fig. 5), although a chi-squared comparison of NISP and MNE by
736 body portion found these two quantitative units to be statistically indistinguishable (χ^2 = 7.673,
737 p = 0.175). Non-ungulate taxa, and in particular reptiles, carnivores, and elephant, are best
738 represented by axial elements, whereas birds are well-represented by elements of the forelimb.

739 Ungulates are best represented by the appendicular skeleton, and more specifically small- and
740 medium-sized ungulates by elements of the forelimb and distal limb, respectively. Moreover,
741 a number of medium-sized ungulate limb bones were complete: three radii (50% of MNE), two
742 tibiae (18% of MNE), three metacarpals (33% of MNE), and two metatarsals (25% of MNE).
743 We focus the discussion of skeletal part survivorship on ungulates as they make up the bulk of
744 the Unit 5 assemblage and because there has been much research dedicated to understanding
745 how post-depositional processes affect ungulate skeletal remains.

746 ***### PLACE FIGURE 5 AROUND HERE***

747 No correlation was found between small-sized bovid limb bone representation and goat
748 bone mineral density (Table 6, data from Tables S3). Although the sample size is very small,
749 it is consistent with the abovementioned evidence for limited fragmentation of small animal
750 remains. A significant positive correlation was found when comparing medium-sized bovid
751 limb bone survivorship and wildebeest bone mineral density, indicating that a significant
752 portion of the assemblage has undergone density-mediated attrition. This correlation is
753 underscored by the presence of 39 dense midshaft fragments that could not be confidently
754 attributed to a specific limb bone but that probably belong to medium-sized ungulates. No
755 correlation was found between small- or medium-sized ungulate element survivorship and
756 SFUI (Table 6, data from Table S4), suggesting that bone density, rather than economic utility,
757 better explains the observed skeletal part profile in the Unit 5 deposit.

758 All Voorhies' transport groups are well-represented in the Unit 5 fossil assemblage,
759 suggesting that overall the assemblage has not been significantly influenced by hydraulic
760 sorting (Fig. 6). This is also supported by the tooth to vertebra ratio which falls within the range
761 reported by Behrensmeyer (1975) for limited or no hydraulic sorting. However, a closer
762 inspection of the southern and northern trenches identified clear differences in the

representation of easy and difficult to transport elements between the two areas. Figure 6 illustrates that easily transported elements are more common in the southern than the northern part of the site and a chi-squared test found the two areas differed significantly ($\chi^2 = 14.136$, $p = 0.007$). This is also borne out by the tooth to vertebra ratios (Fig. 8), which also differ significantly between the two areas ($\chi^2 = 16.326$, $p < 0.001$). This suggests that the southern and northern trenches represent transported and lag deposits, respectively. It seems possible that lake level fluctuations spatially arranged elements in the landscape, which, in this instance, appears to have redeposited easy to transport elements further south.

PLACE FIGURE 8 AROUND HERE

5.4.3 Bone surface modifications – abiotic modifications

Weathering of the Unit 5 fossils ranged from Behrensmeyer's (1978) stage 0–4 with the bulk of the fossils exhibiting stages 0–2 (Fig. 7). Assuming a semi-arid grassland setting similar to the Amboseli National Park, Kenya, most of the bones in this study would have been exposed for 0–6 years prior to burial, while some were perhaps exposed for more than ten years (Behrensmeyer, 1978, Table 2). Such a varied weathering pattern is not uncommon in open-air bone assemblages (e.g. Behrensmeyer, 1978; Tappen, 1995; Hutson, 2012), and, in this instance, probably reflects a prolonged accumulation of bones which were variably affected by sub-aerial weathering through time. Stimpson et al. (2016) previously noted that the fossils from the southern part of the site were less weathered than those from the northern part of the site and a statistical analysis incorporating new material supports this assertion ($\chi^2 = 10.512$, $p = 0.032$). However, this difference disappears when examining medium-sized animals only ($\chi^2 = 8.878$, $p = 0.064$), and, therefore, it appears that this difference is largely driven by the more abundant small animal remains in the southern trenches. Indeed, it is clear from a visual inspection of weathering stages that small-sized animals are less weathered than medium- and

large-sized animals (Fig. 7), while a test for correlation found that fossil size and weathering stage were significantly and positively correlated ($r = 0.183$, $p < 0.001$; $r_s = 0.249$, $p < 0.001$). More rapid burial of smaller bones, possibly facilitated by lake level fluctuations, probably accounts for the differences in weathering, and similar observations have been made elsewhere (Andrews and Whybrow, 2005). Rodent gnawing, manganese staining, and sedimentary abrasion of the Unit 5 assemblages was negligible. Root etching was occasionally observed indicating the deposition of the bones in vegetated soils.

PLACE FIGURE 7 AROUND HERE

5.4.4 Bone surface modifications – butchery and tooth marks

Roberts et al. (2018) reported, in addition to lithic artefacts, medium-sized animal ribs and long bones bearing marks reminiscent of cut and hammerstone percussion marks, suggesting that hominins were likely butchering animals at the site, and a complete list of tooth-marked and probably butchered specimens according to element is provided in Tables S5 and S6. During the present analysis, we identified an additional specimen – an adult elephant rib (SGS-NEFUD-108; Fig. 8G) recovered from the Elephant Quarry – bearing several parallel linear grooves reminiscent of cut marks on its ventral face and similar to those reported by Roberts et al. (2018). The markings are bidirectional and run roughly perpendicular to the long axis of the rib. Two of the markings have a deep V-shaped cross-section and exhibit clear shoulder effect, while the others are more surficial. The presence of these markings on the ventral side of the rib suggests that if they are genuine cut marks that they were produced during evisceration, and similar markings have been found on elephant ribs at other middle Pleistocene zooarchaeological sites (e.g. Áridos 2, Spain; Yravedra et al., 2010).

Carnivore tooth marks were commonly observed (18.3% of NISP) and included pits (*n*=10), scores (*n*=17), punctures (*n*=38), and furrowing of cancellous bone (*n*=38; Fig. 8A-C).

Comparable abundances of tooth-marked bones have been observed in modern landscape assemblages in the Park National des Virunga, Democratic Republic of Congo, an area inhabited by non-migratory ungulates, lions, spotted hyena, and leopards (~15%; Tappen et al., 2007). Higher abundances of tooth-marked bones were observed in the Ngamo Pan, Zimbabwe (~42%; Hutson, 2012), and in mostly lion-accumulated carcasses in the Maasai Mara National Park, Kenya (~42%; Domínguez-Rodrigo, 1999), while similar or higher abundances still are typically encountered in carnivore dens (Pickering, 2002; Kuhn et al., 2010). Examining skeletal elements by body portion revealed that limb bones are most frequently gnawed – in the order of hindlimbs (50.0% of NISP), distal limbs (45.6% of NISP), and forelimbs (31.9% of NISP) – followed by elements of the feet (20.0% of NISP), axial (19.6% of NISP), and lastly the cranium (9.2% of NISP). Ribs, too, are frequently gnawed (29% of NISP) which is unsurprising given that these elements are often damaged/destroyed early in the consumption sequence by carnivores during evisceration (Blumenschine, 1986; Domínguez-Rodrigo, 1999). According to body-size, medium-sized animals are most frequently gnawed, followed by small- and large-sized animals (Table 2).

Carnivore diversity in the Unit 5 fossil assemblage suggests that several species may have played a role in the accumulation of the fossil assemblage (see Table S1). Of these, the large-bodied pantherine (*Panthera* sp. cf. *P. gombaszoegensis*) and hyena (cf. *Crocuta crocuta*) are the only capable hunters of medium- and large-sized prey and likely contributed greatest to the accumulation of bones at the site. Canids typically target smaller and more juvenile prey (Stiner, 1990), but like hyena they are highly destructive of bone and exhibit some degree of osteophagy (Sala et al., 2014), and, therefore, may have also significantly impacted the Unit 5 fossil assemblage. Small carnivores (mustelids, *Vulpes*) were the likely predators of smaller animals such as birds, reptiles, and rodents, and may have also scavenged from the refuse of larger carnivores. To elucidate the role of carnivores in accumulation of the Unit 5 fossil

assemblage, we compared tooth mark frequency to actualistic and landscape studies modelling hominin and carnivore feeding behaviours. We focus the discussion on medium-sized animal limb bones (not including the scapula or pelvis) and limb bone units (epiphyses, midshafts) as damage to these elements has been shown to be highly sensitive to hominin-carnivore-carnivore interactions during carcass processing (e.g. Blumeschine, 1988, 1995; Capaldo, 1997; Faith and Behrensmeyer, 2006; Faith et al., 2007; Gidna et al., 2014).

The number of tooth-marked limb bones falls between experimental scenarios modelling carnivore primary and secondary access to carcasses (Fig. 9): there are fewer tooth-marked limbs bones than observed in assemblages generated by hyenas with primary access to carcasses or secondary access to defleshed but unbroken bones (HI, WBH); more tooth-marked limb bones than observed in experimental settings where hyenas had access to only defleshed and demarrowed bones (HHI, HHII); more tooth-marked limb bones than observed in assemblages generated by lions with primary access to carcasses (LI, LII); and more tooth-marked limb bones than in experimental scenarios modelling hominin secondary access following lion processing (LH). Breaking down limb bones into epiphysis and midshaft portions revealed that the epiphyses are more frequently gnawed than the midshafts. The number of gnawed epiphyses is consistent with primary accumulation by lions, but the number of gnawed midshafts falls outside the range for primary accumulation by lions and is consistent with experimental scenarios modelling hyena secondary access to defleshed and demarrowed bone. In this scenario, midshafts are for the most part ignored by hyenas as they offer little nutritional value once hominins have exploited the within bone nutrients (Blumenschine, 1988; Capaldo, 1997). However, as there is limited evidence to suggest that hominins were processing carcasses on-site, a strict hominin-carnivore model of carcass consumption is not currently supported, although some scavenging from hominin kills may have, in fact, occurred. Breaking down limb bones by element found that the femur is the most gnawed limb bone

(100% of NISP), followed by the tibia (77% of NISP), radius (40% of NISP), metapodials (37% of NISP), ulna (33% of NISP), and lastly the humerus (17% of NISP). The hind quarters of ungulates are highly nutritious – because of the large amount of flesh and marrow that they bear – and, as a result, are typically the first and often most intensively processed part of the carcass (Blumenschine, 1986; Organista et al., 2016). Intensive processing or transport of the hind quarter would also explain the near-absence of highly nutritious femoral remains, as well as the scarcity of the proximal, but not distal, tibia. While the scarcity of tooth-marked humeri is difficult to reconcile, the lack of highly nutritious proximal humeri epiphyses can probably be attributed carnivore processing. Moderate damage of the metapodials is consistent with the low nutritional value of these elements. Carnivore damage differed between the southern and northern trenches ($\chi^2 = 21.610$, $p < 0.001$) with those from the latter being significantly more gnawed (Table S6). This statistical difference remained when considering only medium-sized animals ($\chi^2 = 5.844$, $p = 0.015$), and, as such, it appears that carnivore processing was more intense in the northern part of the site.

The maximum length and breadth measures for tooth pit and puncture size across all skeletal elements ranged from 2.6–16.3 mm (mean=6.0 mm, *n*=41) and 1.1–16.3 mm (mean=4.3, *n*=43), respectively. The average tooth mark dimensions most closely resemble tooth pits produced by large carnivores on limb bone epiphyses and shafts, namely by lions, hyenas, and large canids (Domínguez-Rodrigo and Piqueras, 2003; Delaney-Rivera et al., 2009; Sala et al., 2014). Some of the smaller tooth pits may have been produced by smaller carnivores (e.g. *Vulpes*) and gnawing of bird birds can probably be attributed to these smaller carnivores (e.g. Stimpson et al., 2016, Fig. 6E).

PLACE FIGURE 8 AROUND HERE

PLACE FIGURE 9 AROUND HERE

5.4.5 Mortality profile

Mortality profile analysis focuses on medium-sized bovids as the sample size for the other size classes was too small, and we include material collected from the Elephant Quarry (*n*=4) to boost the sample size. According to the relative abundances of each age class, prime-adults (MNI=8) are most abundant, followed by juveniles (MNI=7, young juveniles MNI=4, subadult juveniles MNI=3), and lastly old individuals (MNI=3). When plotted, the Unit 5 mortality data falls within the living structure space on the ternary plot (Fig. 10). Plotting the 95% confidence intervals found no differences between mortality profiles of medium-sized ungulates from Unit 5 and those killed by wolf (*Canis lupus*), hyena (*Crocuta crocuta*), and lion (*Panthera leo*), but a significant difference between the African wild dog-killed (*Lycaon pictus*) wildebeest mortality profile which comprises almost entirely of young juveniles (Fig. 10A). Chi-squared and Fisher's exact test demonstrate significant differences between the Unit 5 mortality data and those of African wild dog and hyena (Table 7). When plotted, the Unit 5 95% CI overlapped with both ambush and cursorial predators, although only just with the latter (Fig 10B), while chi-squared tests found that the Unit 5 differed significantly from cursorial predators only (Table 7). Comparisons with ethnographic observations of modern hunter-gatherer hunts (i.e. Hadza, Kua) and mortality data for various African open-air Pleistocene archaeological sites found no differences (Fig. 10C; Table 7). The Unit 5 assemblage sample size is, however, too small to identify any definitive patterns in mortality – that is, the density contours are large and cross into the attritional structure, living structure, and prime-dominated spaces of the ternary plot. Nonetheless, the mortality profile is most consistent with predation by hominins and some non-hominin carnivores, notably ambush predators (e.g. lion), and may reflect the use of ambush predation strategies at a watering hole. On the face of it, this suggest that there may have been a significant amount of vegetative cover around the lake to facilitate hunting by ambush, although additional palaeoenvironmental and palaeobotanical evidence

would be needed to test this hypothesis. The abundance of small fragile animal remains (birds, reptiles, rodents) and number of young-juvenile ungulate remains in the Unit 5 assemblage suggests that a bias against young juveniles was likely minimal. Nevertheless, we conducted the above analyses excluding young juvenile remains and found results to be broadly similar, although with a greater degree of confidence interval overlap and larger *p*-values across almost all pairwise comparisons (Fig. 10D–F).

5.5 Initial taphonomic observations of the TAG Sandstone Ridge (TSR), Iron Lake (TIL), and Lake Surface (TLS) fossil assemblages.

Surveys in the TAG basin recovered a wealth of fossiliferous material from two of the three investigated surface deposits: TSR and TLS. The fossil assemblages are poorly preserved and heavily fragmented but differ from one another – notably in their appearance and degree of preservation – suggesting rather distinct taphonomic histories. Very few taxa could be confidently identified (Table S1), and it appears that much of the material is attributable to a medium-sized ungulate. *Oryx* was the only medium-sized ungulate identified, as represented by numerous maxillae, mandible, and horn core specimens, and, as such, we believe that a significant portion of these assemblages probably belong to this genus. Small-sized animals include at least one other smaller bovid species, as well as tortoise, while elephant was the only large-sized animal identified, as represented by a few tooth enamel specimens. We discuss our initial taphonomic observations of each of these assemblages with the caveat that they were collected during pedestrian surveys, and, therefore, are likely biased towards larger, more easy-to-spot fossil specimens, as is implied by the specimen length profiles which comprise few of the smallest fossils (Fig. S6). The results of the quantitative taphonomic analysis and complete skeletal part representation of the TSR and TLS assemblages are provided in Tables S7 and S8, respectively.

The shaft ratio for both assemblages is near consistent with those generated by hyena and hominins under experimental settings and most closely matches those produced by hyenas with primary access to carcasses (Table 5). Chi-square test comparisons found no statistical difference between the TSR assemblage and the hyena-only model, while all other comparisons were found to differ significantly. These differences appear largely driven by the greater number of Type 2 and Type 3 long bone midshafts in the experimental datasets when compared to the TSR and TLS assemblages. While carnivore processing may be responsible for the degree of fragmentation in these assemblages, it's possible that abiotic post-depositional destruction processes (e.g. post-burial attrition, salt weathering) also contributed, and the abundant dry-fracture bone in each of the assemblages supports this assertion. Such processes appear to have been more pronounced in the TLS assemblage, as evidenced by the significantly greater number of dry-fractured bone ($\chi^2 = 12.914$, $p < 0.001$), coupled with the relatively fewer Type 2 and Type 3 long bone midshafts (Table S7) and smaller fossils (Fig. S6). Still, there is an abundance of green-fractured bones in each of these assemblages, attesting to the role of biotic agents in its accumulation and fragmentation, as well as intermediately fractured midshafts, indicating that long bone fragmentation occurred at various points in the history of the deposit. The hyper-abundance of midshafts, which are among the densest portion of the vertebrate skeleton (Lam et al., 1998, 1999), suggests strong density-mediated attrition of these assemblages. Moreover, it’s possible that post-fossilisation processes, such as salt and insolation weathering, have further degraded the fossil assemblages. Indeed, much of the fragmentary geological material that fills the western Nefud Desert is thought to be the result of such processes (Edgell, 2006).

The analysis of bone surface modifications was complicated by significant polish, rounding, surficial pitting, and some larger “comet like” pitting consistent with abrasion by fine wind-blown sand (Fig. S7; d’Errico, 1984; Fernandez-Jalvo and Andrews, 2016, Fig.

A.119). Although the number of wind-abraded specimens was not precisely recorded, we note that the clear majority of fossils exhibited some degree of polish and/or rounding (e.g. Fig. 8F). Therefore, any reading of the bone surface modifications of the assemblages should bear in mind that wind abrasion has likely obscured or removed much of the bone surface information. Nevertheless, it is possible to make some preliminary inferences regarding the taphonomic history of these assemblages from the bone surface modification data at hand.

The weathering profiles, which include unweathered and extensively weathered fossils, indicate that while some bones were buried rather rapidly, others were likely exposed for upwards of ten years, or were repeatedly exposed (see Behrensmeyer, 1978, Table 2). Again, this likely represents a prolonged accumulation of bones variably affected by weathering in an open-air setting. The two weathering profiles were found to differ significantly ($\chi^2 = 15.06$, $p = 0.01$) with relatively more stage 3 and stage 4 bones present in the TLS assemblage. The physiochemical stresses associated with weathering degrade bone and promote fragmentation (Hutson, 2018) and the more severe weathering of the TLS fossils would help to explain the relatively greater number of highly fragmented long bone midshafts and dry-fractured bones. No evidence of root etching, rodent gnawing, or staining, and very little evidence for sedimentary/trampling abrasion was observed.

Carnivore tooth-marked bone and hyena coprolites suggest that carnivores played at least some role in the accumulation of the assemblage, consistent with the degree of long bone fracturing and abundance of green-fractured bone. Also, there is tentative evidence to suggest that hominins, too, may have played a role in the accumulation and modification of the TSR assemblage: a medium-sized animal midshaft fragment with curved, smooth, and oblique fracture pattern, large flake scar with ripple marks, and a single angled V-shaped and slightly curved groove with subtle shoulder effect reminiscent of a cut mark (Fig. 8D); two medium-sized animal and one large-sized animal midshaft fragments with large arcuate notches with

corresponding medullary conchoidal flake scars are most consistent with those generated by hammerstone percussion (Fig. 8E–F); one of these midshafts has two notches with corresponding cortical flake scars (Fig. 8E); while another has an impact scar on the fracture surface opposite the negative flake scar suggestive of breakage and use of an anvil (Fig. 8F).

Only fourteen fossils were collected from the TIL area; nine of these displayed preservation and colour characteristics similar to that of the TLS fossils and were excluded, leaving five specimens confidently assigned to the TIL deposit. The only two identifiable bones were long bone shaft fragments, and it appears that all specimens are from very large mammals. The fossils exhibit significant exfoliation and exposure of underlying cancellous bone, although they appear to be less rounded than fossils from the other two assemblages. Future systematic excavation of the TIL palaeolake may yield fossiliferous material suitable for detailed zooarchaeological and taphonomic analyses.

5.6 Lithic analysis

With the caveat that the new lithics assemblages are small, and those for TIL and TSR are very small, we describe the basic features of the new assemblages. No large cutting tools (e.g. handaxes) have been found in the TAG basin, nor diagnostic debitage associated with their production (e.g. biface thinning flakes). Likewise, diagnostically young features, such as high levels of exotic raw materials and arrowheads, are absent. The overall features of all assemblages are consistent with a Middle Palaeolithic attribution. In total, 156 lithic artefacts were recovered: 12 from TIL, 10 from TSR, and 134 from TLS.

The basic typological features of the assemblages are listed in Table 8. All assemblages are dominated by flakes, which (excluding Levallois flakes) make up between 75 and 63% of the assemblages. Levallois flakes are relatively common. Retouched tools are only present in the TLS assemblage, where they make up a relatively large proportion of the assemblage

compared to other Middle Palaeolithic assemblages. Levallois cores are present in the TLS assemblage, but non-Levallois cores are common. Chips and chunks are present in very low frequencies. These technological features suggest a coherent character to hominin behaviour. They indicate the import of lithics to the site, as indicated by high frequencies of Levallois flakes and, in the TLS assemblage, retouched flakes.

The Levallois flakes and cores present a consistent insight into the character of the reduction process. Striking platforms are generally facetted, and debitage surfaces were prepared centripetally. Both centripetal preferential and recurrent Levallois cores are present. A single exception is a Levallois point/triangular flake with unidirectional convergent preparation from TLS. Non-Levallois cores are either multiplatform or single platform. These may indicate some chronological variation in the samples but are also not inconsistent with a Middle Palaeolithic attribution for all of the material. The retouched artefacts are generally rather basic laterally, and sometimes distally, retouched flakes.

Table 9 summarise the raw material used in the assemblages. The main materials used were different forms of quartzites. This is similar to other sites in the area (Breeze et al., 2017; Groucutt et al., 2017; Groucutt et al., 2018). Ferruginous quartzites are generally found in iron rich horizons within the sandstones in the Nefud region. Other forms of quartzites appear to occur as generally rounded pebbles, of either fluvial or conglomeritic origin. Our surveys in the area suggest that ferruginous quartzite exposures, which are the key raw material source for most Pleistocene sites in the region (*ibid*), are sparse in the area close to TAG. This may correlate with the frequent use of chert, which is of a poor quality, lacustrine form that is found outcropping locally. The only other site identified in the Nefud where this chert was also used in high frequencies is the site of Al Wusta, three kilometres from TAG, where similar low-quality chert is the most common raw material used (Groucutt et al., 2018). This paucity of good raw material in the area may explain some of the characteristics of the TLS assemblage,

where Levallois flakes and retouched tools are present in quite high frequencies. This suggests that these were curated objects, carried into the dune field.

Table 10 summarises mean average values for basic metric features of flakes in each assemblage, as a way to offer a basic summary of the size and shape of the TAG lithics. This both highlights the basic similarities between the sizes of flakes in the different assemblages, and also indicates the generally small size of flakes. The small average size of flakes also demonstrates the systematic nature of the survey transects. Small flake size also suggests that relatively small clasts were being worked, and relatively small artefacts transported to the site. In fact, the TAG flakes are very short for a Middle Palaeolithic assemblage – being shorter than those from Middle Palaeolithic sites such as Tor Faraj, Warwasi (layers WWXX), JKF-1 and Porc Epic (Groucutt, 2014). However, the flakes are on average thicker than in all of these assemblages, and wider than most of them. The knappers at TAG were generally producing relatively thick and squat flakes. The mean average for elongation (length/width) at TAG is 1.3, which is very squat for a Middle Palaeolithic assemblage – flakes at Tor Faraj and Porc Epic have average values of 2.1 and 2, respectively (Groucutt, 2014). These features probably reflect a combination of both raw material and technology.

The newly recovered lithics were found relatively evenly distributed across the surveyed areas, and not in discrete 'knapping scatters'. While their distribution may have been influenced by taphonomic processes, it is also parsimonious that they represent artefacts abandoned during repeated hominin visits to the locality.

6. Discussion

Ti's al Ghadah is the most significant Pleistocene palaeontological site in Arabia, and this is further underscored in the current study by the identification of new fossil- and artefact-bearing deposits that relate to temporally discrete phases of lake formation within the Ti's al

Ghadah basin. Previous analyses of the Unit 5 fossil deposit have identified a diverse suite of fauna illustrative of semi-arid grassland conditions, evidence for carnivore processing of bone, and the earliest traces of hominin activity in Arabia in the form of lithic artefacts and probably butchered bone (Thomas et al., 1998; Scerri et al., 2015; Stimpson et al., 2015, 2016; Roberts et al., 2018). The current study presents a detailed taphonomic assessment of this site in an effort to determine the main bone accumulation processes and elucidate the relative roles of hominins, carnivores, and environment in the formation of the assemblage. In turn, this provides a unique insight into the palaeoecology of the Arabian Peninsula during middle Pleistocene.

The Unit 5 assemblage is well-preserved and appears to have undergone minimal post-depositional destruction, as evidenced by the recovery of complete fragile skeletal elements, abundant small bird, rodent, and reptile remains, limited fragmentation of long bone midshafts, and the discovery of bones in semi-articulated states. The northern part of the site is far less taxonomically rich, and this may relate to the preferential transport of small-sized animal remains driven by lake level fluctuations. Indeed, Rosenberg et al. (2013) noted that the facies associated with the palaeolake sediments overlying Unit 5 were characteristic of a near-shore position within the lake. Preferential transport is also supported by the Voorhies transport group analysis that found easy to transport elements were more concentrated in the southern trenches. If bones were fluvially transported, the lack of evidence for rounding and sediment abrasion suggests that this occurred in a low energy environment consistent with a lake shore.

Carnivores contributed at least partially to the accumulation and modification of the Unit 5 fossil assemblage, as evidenced by tooth-marked and green-fractured bone, and their presence is confirmed by the discovery of carnivore remains and coprolites (Thomas et al., 1998; Stimpson et al., 2015, 2016; Roberts et al., 2018). The skeletal part representation and distribution of carnivore tooth marks is broadly consistent with processing by large carnivores

– that is, highly nutritious elements (e.g. ribs, femur, pelvis) are commonly gnawed and highly nutritious element portions (e.g. proximal humerus, proximal femur) are generally underrepresented in relation to less nutritious elements (cf. Blumenschine, 1986; Marean and Spencer, 1991; Marean et al., 1992; Domínguez-Rodrigo, 1999; Faith and Behrensmeyer, 2006; Faith et al., 2007). The number of tooth-marked limb bones falls between experimental models of carnivore primary and secondary access to carcasses following processing by hominins but is near consistent with the latter. However, a strict hammerstone-carnivore model of bone accumulation is at odds with the abundance of Type 3 long bones, as well as the scarcity of even tentatively assigned butchery marks. For example, Capaldo (1997) found that in assemblages first processed by hominins and subsequently scavenged by hyenas that 13–23% and 9–25% of medium-sized animal limb bones retained cut and percussion marks, respectively. Similarly, Blumenschine and Selvaggio (1998) noted in their hammerstone processing experiments that roughly one third of the resulting limb bone fragments bore at least one percussion mark.

Alternatively, the low number of tooth-marked long bones may reflect primary access to carcasses by large felids, which is also supported by the abundance of Type 3 long bones and the living structure mortality profile (although the latter is also consistent with a number of zooarchaeological assemblages). Felids are specialised flesh-eaters with teeth especially designed for meat slicing, and, as a result, generate comparatively fewer tooth marks and broken bones during carcass processing than do more durophagous carnivores like hyenas and canids (Turner and Anton, 1997; Domínguez-Rodrigo et al., 2007; Pobiner, 2007; Gidna et al., 2014; Arriaza et al., 2016; Aramendi et al., 2017). Indeed, the number of tooth-marked epiphyses falls within the range observed in modern landscape assemblages accumulated by wild lions (Fig. 9). The survival of a number of complete long bones and axial elements also points to a large felid as the primary accumulator of bones at the site. The number of tooth-

1107 marked midshafts and abundant green-fractured bones is, however, at odds with carcass
1108 processing by large felids only and suggests that more durophagous carnivores on occasion
1109 scavenged from large felid kills. However, we cannot discount that the large felid identified in
1110 the Unit 5 assemblage (*Panthera* sp. cf. *P. gombaszoegensis*) had a different feeding behaviour
1111 to extant analogues. Indeed, during the Pleistocene an evolutionary trend in large felids from a
1112 "chewing" dentition to one more specialised for "meat-slicing" has been reported, and among
1113 the Pleistocene pantherines *Panthera gombaszoegensis* was particularly well-adapted to bone
1114 crushing (Hemmer et al., 2010; Diedrich, 2013). Moreover, jaguars (*Panthera onca*), which
1115 are thought to be closely related to the extinct *Panthera gombaszoegensis* (Turner and Antón,
1116 1997), have recently been shown to inflict damage to bones that are more comparable with
1117 durophagus carnivores such as hyena (Rodríguez-Alba et al., 2019). Nonetheless, the direct
1118 fossil evidence for hyenas and canids, significant density-mediated attrition among medium-
1119 sized ungulate limb bones, and abundant green-fractured long bones suggest that these
1120 carnivores played some role in the modification of the Unit 5 assemblage and similar
1121 frequencies of tooth-marked midshafts have been observed in the FLK North 3 and FLK North
1122 4 fossil assemblages (Olduvai Gorge, Tanzania), two sites thought to be accumulated by large
1123 felids and intermittently scavenged by hyenas (Domínguez-Rodrigo et al., 2007a). Smaller
1124 carnivores such as foxes (*Vulpes* sp.) and mustelids, as well as non-mammalian carnivores such
1125 as vultures (*Neophron percnopterus*) and varanids, may have also scavenged from large
1126 carnivore refuse, and are probably responsible for the accumulation of small bird, reptile, and
1127 rodent remains at the site. The presence of vultures implies limited or no tree/bush cover
1128 (Domínguez-Rodrigo, 2001) and suggests that ambush hunting at the lakeside was probably
1129 facilitated by high grasses. Hunting at the site was focused on medium-sized ungulates, most
1130 notably oryx and equids. Lions are specialist hunters that preferentially target a narrow range
1131 of medium-sized ungulate taxa, whereas hyena are generalist predators that take a wider range

of prey/scavenged species (Hayward and Kerley, 2005; Hayward, 2006). The relative abundance of oryx remains at the site is therefore consistent with accumulation by a specialist carcasses collector (e.g. lion).

Hominins may have also engaged in scavenging at Unit 5, as large felids occasionally leave a considerable amount of scavangeable flesh and within bone tissue following carcass processing (Pobiner, 2007). However, if the two ungulate ribs detailed in Roberts et al. (2018) and the elephant rib described in the present study represent genuine cut-marked bones, it would suggest that hominins had, at least on occasion, primary access to medium- as well as large-sized animal carcasses as these elements are quickly destroyed by carnivores during evisceration (Blumenschine, 1986; Domínguez-Rodrigo, 1999). If hominins were actively hunting in the western Nefud Desert, the low anthropogenic signal in the Unit 5 fossil assemblage may be explained by off-site carcass processing – as proposed by the "near-kill location" and "refuge" models (Blumenschine, 1991; Blumenschine et al., 1994; O'Connell, 1997; O'Connell et al., 2002). These models posit that early hominins transported carcasses, or some portion of them, away from kill sites (often surrounding rivers and lakes) to nearby protected areas to avoid/delay competition with other carnivores; a method employed by modern hunter-gatherer groups (e.g. Hadza [Bunn et al., 1988; O'Connell et al., 1992]). Given the open grassland lakeshore setting, and the presence of large and potentially dangerous carnivores, hominins in the western Nefud may have benefited from such a subsistence strategy.

In contrast to the Unit 5 assemblage, the surface fossil deposits (TSR, TIL, TLS) assessed here are poorly preserved and heavily fragmented, and, as such, far less can be reliably said about their accumulation. Wind abrasion has affected much of these assemblages, while other attritional processes such as salt and insolation weathering may have further degraded the fossils. We note that some of the ungulate teeth in the TSR assemblage were exceptionally

worn, in some cases surpassing the cementoenamel junction. Behrensmeyer et al. (2012) noted that severe drought in Amboseli National Park resulted in extensive tooth wear in ungulates owing to their grittier diet. Carnivores played at least some role in the accumulation of these assemblages, and it seems likely that their role was greater than the current bone surface modification data suggests. Lastly, we note that hominins, too, may have played a role in the accumulation of the TSR assemblage, as suggested by notches and grooves redolent of cut and hammerstone percussion marks. The recovery of lithic artefacts alongside fossils evokes hominins as potential accumulators of fossils around the lake at Ti's al Ghadah. Significantly, the lithic artefact assemblages associated with various phases of lake formation indicated repeated use of the Ti's al Ghadah basin by hominins during pluvial phases of the Pleistocene and, as previously stated by Scerri et al (2015), may represent the earliest Middle Palaeolithic assemblage in Arabia.

7. Conclusions

The Unit 5 assemblage of Ti’s Al Ghadah, and accompanying sedimentological evidence, suggest that the deposit represents a serial predation hotspot where large felids and probably hominins ambushed mostly medium-sized ungulates in a lakeside environment, while more durophagous carnivores such as hyenas and canids occasionally scavenged from large felid kills. Less can be said about the other assemblages present in the basin, but the evidence preserved suggest that they too were accumulated by, at the very least, non-hominin carnivores in a lakeside environment. This study provides the first detail insights into the interplay between hominins, carnivores, and herbivores in Arabia, and suggests that watering holes have been a focus on the Arabian landscape for resources since the middle Pleistocene.

Acknowledgements

Our work in Saudi Arabia is supported by His Royal Highness Prince Sultan bin Salman, President of the Saudi Commission for Tourism and National Heritage (SCTH). Financial support for our research has been provided by the European Research Council (grant no. 295719, to MDP), the Max Planck Society and the SCTH. We thank Darrin Lunde and John Ososky from the Smithsonian Institution for providing access to the vertebrate collection and Louise Martin for providing comparative morphometric data. We would also like to thank Karen Privat at the Mark Wainwright Analytical Centre (UNSW) for assistance with SEM imaging. MS would like to thank The Leakey Foundation and PANGEA Research Centre (UNSW) for funding. HSG thanks the British Academy for funding. JL is supported by an Australian Research Council Future Fellowship (FT160100450). AMA thanks the Research Centre at the College of Tourism and Archaeology, King Saud University for their support.

Appendix A. Supplementary material

Supplementary data related to this article can be found online at

Competing interests

The authors declare no competing interests.

References

Andrews, P., Whybrow, P., 2005. Taphonomic observations on a camel skeleton in a desert environment in Abu Dhabi. Palaeontologia Electronica 8 (1).

Aramendi, J., Uribelarrea, D, Arriaza, M.C., Arráiz, Barboni, D., Yravedra, J., Ortega, M.C., Gidna, A., Mabulla, A., Baqeudano, E., Domínguez-Rodrigo, M., 2017. The paleoecology and taphonomy of AMK (Bed I, Olduvai Gorge) and its contributions to the understanding of the "Zinj" paleolandscape. Palaeogeography, Palaeoclimatology, Palaeoecology 488, 35–49.

Armitage, S.J., Jasim, S.A., Marks, A.E., Parker, A.G., Usik, V.I., Uerpmann, H.-P., 2011. The Southern Route "Out of Africa": Evidence for an Early Expansion of Modern Humans into Arabia. Science 331, 453–456.

Arriaza, M.C., Domínguez-Rodrigo, M., Yravedra, J., Baquedano, E., 2016. Lions and bone accumulators? Palaeontological and ecological implications of a modern bone assemblage from Olduvai Gorge. PLoS ONE 11(5): e0153797.

Bar-Oz, G., Munro, N., 2004. Beyond cautionary tales: a multivariate taphonomic approach for resolving equifinality in zooarchaeological studies. Journal of Taphonomy 2, 202–222.

Battarbee, R.W., Kneen, M.J., 1982. The use of electronically counted microspeheres in absolute diatom analysis. Limnology and Oceanography 27, 184-188.

Behrensmeyer, A.K., 1975. Taphonomy and paleoecology in the hominid fossil record. Yearbook of Physical Anthropology 19, 36–50.

Behrensmeyer, A.K., 1978. Taphonomic and ecological information from bone weathering. Paleobiology 4, 150–162.

Behrensmeyer, A.K., Western, D., Badgley, C., Miller, J.H., Odock, F.L., 2012. The impact of mass mortality on the land surface bone assemblage of Amboseli Park, Kenya. Program and Abstracts, Journal of Vertebrate Palaeontology 32, 1–207.

Binford, L.R., 1981. Bones: Ancient Men and Modern Myths. New York Academic Press, New York.

Binford, L.R., 1984. Faunal remains from Klasies River Mouth. Academic Press, Orlando.

Blumenschine, R.J., 1986. Carcass consumption sequences and the archaeological distinction of scavenging and hunting. Journal of Human Evolution 15, 639–659.

1224 Blumenschine, R.J., 1988. An experimental model of the timing of hominin and carnivore influence on
1225 archaeological bone assemblages. Journal of Archaeological Science 15, 483–502.

1226 Blumenschine, R.J., 1991. Hominid carnivory and foraging strategies, and the socio-economic function
1227 of early archaeological sites. Philosophical transactions of the Royal Society 334, 211–221.

1228 Blumenschine, R.J., 1995. Percussion marks, tooth marks, and experimental determinations of the
1229 timing of hominid and carnivore access to long bones at FLK *Zinjanthropus*, Olduvai Gorge,
1230 Tanzania. Journal of Human Evolution 29, 21–51.

1231 Blumenschine, R.J., Cavallo, J.A., Capaldo, S.D., 1994. Competition for carcasses and early hominid
1232 behavioral ecology: A case study and conceptual framework. Journal of Human Evolution 27,
1233 197–213.

1234 Blumenschine, R.J., Selvaggio, M.M., 1988. Percusssion marks on bone surfaces as a new diagnostic
1235 of hominid behaviour. Nature 333, 763–765.

1236 Breeze, P.S., Drake, N.A., Groucutt, H.S., Parton, A., Jennings, R.P., White, T.S., Clark-Balzan, L.,
1237 Shipton, C., Scerri, E.M.L., Stimpson, C.M., Crassard, R., Hilbert, Y., Alsharekh, A., Al-Omari,
1238 A., Petraglia, M.D., 2015. Remote sensing and GIS techniques for reconstructing Arabian
1239 palaeohydrology and identifying archaeological sites. Quaternary International 382, 98–119.

1240 Breeze, P.S., Groucutt, H.S., Drake, N.A., White, T.S., Jennings, R.P., Petraglia, M.D., 2016.
1241 Palaeohydrological corridors for hominin dispersals in the Middle East ~250–70,000 years ago.
1242 Quaternary Science Reviews 144, 155–185.

1243 Breeze, P.S., Groucutt, H.S., Drake, N.A., Louys, J., Scerri, E.M.L., Armitage, S.J., Zalmout, I.S.A.,
1244 Memesh, A.M., Haptari, M.A., Soubhi, S.A., Matari, A.H., Zahir, M., Al-Omari, A., Alsharekh,
1245 A.M., Petraglia, M.D., 2017. Prehistory and palaeoenvironments of the western Nefud Desert,
1246 Saudi Arabia. Archaeological Research in Asia 10, 1–16.

1247 Bunn, H.T., 1982. Meat-eating and human evolution: studies on the diet and subsistence patterns of
1248 Plio-Pleistocene hominids in East Africa. Ph.D. dissertation, University of Wisconsin, Madison.

1249 Bunn, H.T., Bartram, L.E., Kroll, E.M., 1988. Variability in bone assemblage formation from Hadza
1250 hunting, scavenging and carcass processing. Journal of Anthropological Archaeology 7, 412–457.

1251 Bunn, H.T., Kroll, E.M., 1986. Systematic butchery by Plio/ Pleistocene hominids at Olduvai Gorge ,
1252 Tanzania. Current Anthropology 27, 431–452.

1253 Bunn, H.T., Pickering, T.R., 2010. Methodological recommendations for ungulate mortality analyses
1254 in paleoanthropology. Quaternary Research 74, 388–394.

Bunn, H.T., Gurtov, A.N., 2014. Prey mortality profiles indicate that early Pleistocene *Homo* at Olduvai was an ambush predator. Quaternary International 322–323, 44–53.

Cannon, M.D., 2013. NISP, bone fragmentation, and the measurement of taxonomic abundance. Journal of Archaeological Method and Theory 20, 397–419.

Capaldo, S.D., 1997. Experimental determination of carcass processing by Plio-Pleistocene hominids and carnivores at FLK 22 (*Zinjanthropus*), Olduvai Gorge, Tanzania. Journal of Human Evolution 33, 555–597.

Capaldo, S.D., 1998. Simulating the formation of dual-patterned archaeofaunal assemblages with experimental controls. Journal of Archaeological Sciences 25, 311–330.

Capaldo, S.D., Blumenschine, R.J., 1994. A quantitative diagnosis of notches made by hammerstone percussion and carnivore gnawing on bovid long bones. American Antiquity 59, 724–748.

Clark, J.L., 2019. The Still Bay and pre-Still Bay fauna from Sibudu Cave: taphonomic and taxonomic analysis of macromammal remains from the Wadley Excavations. Journal of Paleolithic Archaeology 2. 26–73.

Dechant Boaz, N.T., Behrensmeyer, A.K., 1976. Hominid taphonomy: transport of human skeletal parts in an artificial fluviatile environment. American Journal of Physical Anthropology 45, 53–60.

Delagnes, A., Tribolo, C., Bertran, P., Brenet, M., Crassard, R., Jaubert, J., Khalidi, L., Mercier, N., Nomade, S., Peigné, S., Sitzia, L., Tournepiche, J.F., Al-Halibi, M., Al-Mosabi, A., MacChiarelli, R., 2012. Inland human settlement in southern Arabia 55,000 years ago. New evidence from the Wadi Surdud Middle Paleolithic site complex, western Yemen. Journal of Human Evolution 63, 452–474.

Delaney-Rivera, C., Plummer, T.W., Hodgson, J.A., Forrest, F., Hertel, F., Oliver, J.S., 2009. Pits and pitfalls: taxonomic varability and patterning in tooth mark dimensions. Journal of Archaeological Science 36, 2597–2608.

Delgiudice, G.D., Fieberg, J., Riggs, M.R., Powell, M.C., Pan, W., 2016. A long-term age-specific survival analysis of female white-tailed deer. The Journal of Wildlife Management 70, 1556–1568.

Diedrich, C.G., 2013. Late Pleistocene leopards across Europe – northernmost European German population, highest elevated records in the Swiss Alps, complete skeletons in the Bosnia Herzegowina Dinarids and comparison to the Ice Age cave art. Quaternary Science Reviews 76, 167–193.

1286 Discamps, E., Costamango, S., 2015. Improving mortality profile analysis in zooarchaeology: a revised
1287 zoning for ternary diagrams. Journal of Archaeological Science 58, 62–76.

1288 Domínguez-Rodrigo, M., 1999. Flesh availability and bone modifications in carcasses consumed by
1289 lions: Palaeoecological relevance in hominid foraging patterns. Palaeogeography,
1290 Palaeoclimatology, Palaeoecology 149, 373–388.

1291 Domínguez-Rodrigo, M., 2001. A study of carnivore competition in riparian and open habitats of
1292 modern savannas and its implications for hominid behavioral modelling. Journal of Human
1293 Evolution 40, 77–98.

1294 Domínguez-Rodrigo, M., Barba, R., 2006. New estimates of tooth mark and percussion mark
1295 frequencies at the FLK Zinj site: The carnivore-hominid-carnivore hypothesis falsified. Journal of
1296 Human Evolution 50, 170–194.

1297 Domínguez-Rodrigo, M., Barba, R., Organista, E., 2007a. A taphonomic study of FLK North 3 and 4:
1298 a felid–hyaenid and hominid palimpsest. In: Domínguez-Rodrigo, M., Barba, R., Egeland, C.P.
1299 (Eds.), Deconstructing Olduvai: A Taphonomic Study of the Bed I Sites. Springer, New York, pp.
1300 165–190.

1301 Domínguez-Rodrigo, M., Egeland, C.P., Barba, R., 2007b. The "physical attribute" taphonomic
1302 approach. In: Domínguez-Rodrigo, M., Barba, R., Egeland, C.P. (Eds.), Deconstructing Olduvai:
1303 A Taphonomic Study of the Bed I Sites. Springer, New York, pp. 23–32.

1304 Domínguez-Rodrigo, M., de Juana, S., Galan, A.B., Rodríguez, M., 2009. A new protocol to
1305 differentiate trampling marks from butchery cut marks. Journal of Archaeological Science 36,
1306 2643–2654.

1307 Domínguez-Rodrigo, M., Piqueras, A., 2003. The use of tooth pits to identify carnivore taxa in tooth-
1308 marked archaeofaunas and their relevance to reconstruct hominid carcass processing behaviours.
1309 Journal of Archaeological Science 30, 1385–1391.

1310 Drake, N.A., Breeze, P., Parker, A., 2013. Palaeoclimate in the Saharan and Arabian Deserts during the
1311 Middle Palaeolithic and the potential for hominin dispersals. Quaternary International 300, 48–
1312 61.

1313 von den Driesch, A., 1976. A Guide to the Measurement of Animal Bones from Archaeological Sites.
1314 Peabody Museum Press, Harvard University.

1315 d'Errico, F., Giacobini, G., Ouech, P.F., 1984. Vanish replicas: a new method for the study of worked
1316 bone surfaces. OSSA, 9–11, 29–51.

Faith, J.T., Behrensmeyer, A.K., 2006. Changing patterns of carnivore modification in a landscape bone assemblage, Amboseli Park, Kenya. Journal of Archaeological Science 33, 1718–1733.

Faith, J.T., Marean, C.W., Behrensmeyer, A.K., 2007. Carnivore competition, bone destruction, and bone density. Journal of Archaeological Science 34, 2025–2034.

Faith, J.T., Choiniere, J.N., Tryon, C.A., Peppe, D.J., Fox, D.L., 2011. Taxonomic status and paleoecology of *Rusingoryx atopocranion* (Mammalia, Artiodactyla), an extinct Pleistocene bovid from Rusinga Island, Kenya. Quaternary Research 75, 697–707.

Faith, J.T., Gordon, A.D., 2007. Skeletal element abundances in archaeofaunal assemblages: economic utility, sample size, and assessment of carcass transport strategies. Journal of Archaeological Science 34, 872–882.

Farrant, A.R., Duller, G.A.T., Parker, A.G., Roberts, H.M., Parton, A., Knox, R.W.O., Bide, T., 2015. Developing a framework of Quaternary dune accumulation in the northern Rub' al-Khali, Arabia. Quaternary International 382, 132–144.

Fleitmann, D., Burns, S.J., Neff, U., Mangini, A., Matter, A., 2003. Changing moisture sources over the last 330,000 years in northern Oman from fluid-inclusion evidence in speleothems. Quaternary Research 60, 223-232.

Fleitmann, D., Burns, S.J., Pekala, M., Mangini, A., Al-Subbary, A., Al-Aowah, M., Kramer, J., Matter, A., 2011. Holocene and Pleistocene pluvial periods in Yemen, southern Arabia. Quaternary Science Reviews 30, 783–787.

Gidna, A.O., Kisui, B., Mabulla, A., Musiba, C., Domínguez-Rodrigo, M., 2014. An ecological neo-taphonomic study of carcass consumption by lions in Tarangire National Park (Tanzania) and its relevance for human evolutionary biology. Quaternary International 322–323, 167–180.

Groucutt, H.S., 2014. Middle Palaeolithic point technology, with a focus on the site of Tor Faraj (Jordan, MIS 3). Quaternary International 6, 205–226.

Groucutt, H.S., Breeze, P., Drake, N.A., Jennings, R., Parton, A., White, T., Shipton, C., Clark-Balzan, L., Al-Omari, A., Cuthbertson, P., Wedage, O.M.C., Bernal, M.A., Alsharekh, A., Petraglia, M.D., 2016. The Middle Palaeolithic of the Nejd, Saudi Arabia. Journal of Field Archaeology 41, 131–147.

Groucutt, H.S., White, T.S., Clark-Balzan, L., Parton, A., Crassard, R., Shipton, C., Jennings, R.P., Parker, A.G., Breeze, P.S., Scerri, E.M.L., Alsharekh, A., Petraglia, M.D., 2015a. Human occupation of the Arabian Empty Quarter during MIS 5: Evidence from Mundafan Al-Buhayrah,

Saudi Arabia. Quaternary Science Reviews 119, 116–135.

Groucutt, H.S., Scerri, E.L., Amor, K., Shipton, C., Jennings, R.P., Parton, A., Clark-Balzan, L., Alsharekh, A., Petraglia, M.D., 2017. Middle Palaeolithic raw material procurement and early stage reduction at Jubbah, Saudi Arabia. Archaeological Research in Asia 9, 44-62.

Groucutt, H.S., Shipton, C., Alsharekh, A., Jennings, R., Scerri, E.M.L., Petraglia, M.D., 2015b. Late Pleistocene lakeshore settlement in northern Arabia: Middle Palaeolithic technology from Jebel Katefeh, Jubbah. Quaternary International 283, 215–236.

Groucutt, H.S., Grün, R., Zalmout, I.A.S., Drake, N.A., Armitage, S.J., Candy, I., Clark-Wilson, R., Louys, J., Breeze, P.S., Duval, M., Buck, L.T., Kivell, T.L., Pomeroy, E., Stephens, N.B., Stock, J.T., Stewart, M., Price, G.J., Kinsley, L., Sung, W.W., Alsharekh, A., Al-Omari, A., Zahir, M., Memesh, A.M., Abdulshakoor, A.J., Al-Masari, A.M., Bahameem, A.A., Al Murayyi, K.M.S., Zahrani, B., Scerri, E.L.M., Petraglia, M.D., 2018. Homo sapiens in Arabia by 85,000 years ago. Nature Ecology and Evolution 2, 1–10.

Groucutt, H.S., Petraglia, M.D., 2012. The prehistory of the Arabian Peninsula: Deserts, dispersals, and demography. Evolutionary Anthropology 21, 113–125.

Guagnin, M., Shipton, C., el-Dossary, S., al-Rashid, M., Moussa, F., Stewart, M., Ott, F., Alsharekh, A., Petraglia, M.D., 2018. Rock art provides new evidence on the biogeography of kudu (*Tragelaphus imberbis*), wild dromedary, aurochs (*Bos primigenius*) and African wild ass (*Equus africanus*) in the early and middle Holocene of north-western Arabia. Journal of Biogeography 45, 727–740.

Hammer, Ø., Harper, D.A.T., Ryan, P.D., 2001. PAST: palaeontological statistics software package for education and data analysis. Palaeontologica Electronica 4, 1–9.

Hayward, M.W., 2005. Prey preferences of the spotted hyena (*Crocuta crocuta*) and degree of dietary overlap with the lion (*Panthera leo*). Journal of Zoology 270, 606–614.

Hayward, M.W., Kerley, G.I.H., 2006. Prey preferences of the lion (*Panthera leo*). Journal of Zoology 267, 309–322.

Hemmer, H., Ralf-Dietrich, K., A.K. Vekua. *Panthera onca georgica* spp. nov. from the early Pleistocene of Dmanisi (Republic of Georgia) and the phylogeography of jaguars (Mammalia, Carnivora, Felidae). Neues Jahrbuch für Geologie und Paläontologie, Abhandlungen 257, 115–127.

1378 Hilbert, Y.H., White, T.S., Parton, A., Clark-Balzan, L., Crassard, R., Groucutt, H.S., Jennings, R.P.,
1379 Breeze, P., Parker, A., Shipton, C., Al-Omari, A., Alsharekh, A.M., Petraglia, M.D., 2014.
1380 Epipalaeolithic occupation and palaeoenvironments of the southern Nefud desert, Saudi Arabia,
1381 during the Terminal Pleistocene and Early Holocene. Journal of Archaeological Science 50, 460–
1382 474.

1383 Hoffmann, G., Rupprechter, M., Rahn, M., Preusser, F., 2015. Fluvio-lacustrine deposits reveal
1384 precipitation pattern in SE Arabia during early MIS 3. Quaternary International 382, 145–153.

1385 Hoffstetter, R., Gasx, J.-P., 1969. Vertebrae and ribs of modern reptiles. In: Gans, C., Bellairs, A.d'A.,
1386 Parsons, T.S. (Eds.), Biology of the Reptilia, vol. 1. Academic Press, New York, pp. 201–310.

1387 Holmes, R.B., Murray, A.M., Attia, Y.S., Simons, E.L., Chatrath, P., 2010. Oldest known *Varanus*
1388 (Squamata: Varanidae) from the Upper Eocene and Lower Oligocene of Egypt: Support for an
1389 African origin of the genus. Palaeontology 53, 1099–1110.

1390 Horwitz, L.K., Cope, C., Tchernov, E., 1990. Sexing the bones of mountain-gazelle (*Gazella gazella*)
1391 from prehistoric sites in the southern Levant. *Paléorient* 16, 1–12.

1392 Hutson, J.M., 2012. Neotaphonomic measures of carnivore serial predation at Ngamo Pan as an analog
1393 for interpreting open-air faunal assemblages. Journal of Archaeological Science 39, 440–457.

1394 Hutson, J.M., 2018. The faunal remains from Bundu Farm and Pniel 6: examining the problematic
1395 Middle Stone Age archaeological record within the southern African interior. Quaternary
1396 International 466, 178–193.

1397 Fernández-Jalvo, Y., Andrews, P., 2016. Atlas of Taphonomic Identifications. Springer, Dordrecht.

1398 Jenkins, K.E., Nightingale, S., Faith, J.T., Peppe, D.J., Michel, L.A., Driese, S.G., McNulty, K.P.,
1399 Tryon, C.A., 2017. Evaluating the potential for tactical hunting in the Middle Stone Age: Insights
1400 from a bonebed of the extinct bovid, *Rusingoryx atopocranion*. Journal of Human Evolution 108,
1401 72–91.

1402 Jennings, R.P., Shipton, C., Breeze, P., Cuthbertson, P., Bernal, M.A., Wedage, W.M.C.O., Drake,
1403 N.A., White, T.S., Groucutt, H.S., Parton, A., Clark-Balzan, L., Stimpson, C., al Omari, A.A.,
1404 Alsharekh, A., Petraglia, M.D., 2015. Multi-scale Acheulean landscape survey in the Arabian
1405 Desert. Quaternary International 382, 58–81.

1406 Kahlke, R.-D., Gaudzinksi, S., 2005. The blessing of a great flood: differentiation of mortality patterns
1407 in the large mammal record of the lower Pleistocene fluvial site of Untermassfeld (Germany) and
1408 its relevance for the interpretation of faunal assemblages from archaeological sites. Journal of

1409 Archaeological Science 32, 1202–1222.

1410 Kruuk, H., The Spotted Hyena. University of Chicago Press, Chicago.

1411 Kuhn, B.F., Berger, L.R., Skinner, J.D., Examining criteria for identifying and differentiating fossil
1412 fauna assemblages accumulated by hyenas and hominins using extant hyenid accumulations.
1413 International Journal of Osteoarchaeology 20, 15–35.

1414 Lam, Y.M., Chen, X., Marean, C.W., Frey, C.J., 1998. Bone density and long bone representation in
1415 archaeological faunas: Comparing results from CT and photon densitometry. Journal of
1416 Archaeological Science 25, 559–570.

1417 Lam, Y.M., Chen, X., Pearson, O.M., 1999. Intertaxonomic variability in patterns of bone density and
1418 the differential representation of bovid, cervid and equid elements in the archaeological record.
1419 American Antiquity 64, 343–362.

1420 Louys, J., Meloro, C., Elton, S., Ditchfield, P., Bishop, L.C., 2015. The potential and pitfalls of using
1421 simple dental metrics to infer the diets of African antelopes. Palaeontologica Africana. 49, 8–24.

1422 Lyman, R.L., 1984. Bone density and differential survivorship of fossil classes. Journal of
1423 Anthropological Archaeology 3, 259–299.

1424 Lyman, R.L., 1994. Vertebrate Taphonomy. Cambridge University Press, Cambridge.

1425 Maguire, J.M., Pemberton, D., Collett, M.H., 1980. The Makapansgat limeworks grey breccia:
1426 hominids, hyaenas, hystricids or hillwash? Paleontologica Africana 23, 75–98.

1427 Malnate, E.V., 1972. Observations on the vertebral hypapophyses and associated musculature in some
1428 snakes, with special reference to the Colubridae. Zoologische Mededelingen 47, 225–239.

1429 Marean, C.D., Domínguez-Rodrigo, M., Pickering, T.R., 2004. Skeletal element equifinality in
1430 zooarchaeology begins with method: the evolution and status of the "shaft critique". Journal of
1431 Taphonomy 2, 69–98.

1432 Marean, C.W., Spencer, L.M., 1991. Impact of carnivore ravaging of bone in archaeological
1433 assemblages. Journal of Archaeological Science 18, 667–694.

1434 Marean, C.W., Spencer, L.M., Blumenschine, R.J., Capaldo, S.D., 1992. Captive hyaena bone choice
1435 and destruction, the Schlepp effect and Olduvai archaeofaunas. Journal of Archaeological Science
1436 19, 101–121.

1437 Matter, A., Neubert, E., Preusser, F., Rosenberg, T., Al-Wagdani, K., 2015. Palaeo-environmental
1438 implications derived from lake and sabkha deposits of the southern Rub' al-Khali, Saudi Arabia

1439 and Oman. Quaternary International 382, 120–131.

1440 McClure, H.A., 1984. Late Quaternary Palaeoenvironments of the Rub' al Khali. Ph.D. Thesis,
1441 University College, London.

1442 Metcalfe, D., Jones, K.T., 1988. A reconsideration of animal body-part utility indices. American
1443 Antiquity 53, 486–504.

1444 Mitchell, B.L., Shenton, J.B., Uys, J.C.M., 1965. Predation on large mammals in the Kafue National
1445 Park, Zambia. Zoological Africana 1, 297–318.

1446 Munson, P.J., 2000. Age-correlated differential destruction of bones and its effects on archaeological
1447 mortality profiles of domestic sheep and goats. Journal of Archaeological Science 27, 391–407.

1448 Munson, P.J., Garniewicz, R.C., 2003. Age-mediated survivorship of ungulate mandibles and teeth in
1449 canid-ravaged faunal assemblages. Journal of Archaeological Science. 30, 405–416.

1450 Oliver, J.S., Plummer, T.W., Hertel, F., Bishop, L.C., 2019. Bovid mortality patterns from Kanjera
1451 South, Homa Peninsula, Kenya and FLK-Zinj, Olduvai Gorge, Tanzania: evidence for habitat
1452 mediated variability in Oldowan hominin hunting and scavenging behavior. Journal of Human
1453 Evolution 131, 61–75.

1454 O'Connell, J.F., 1997. On Plio-Pleistocene archaeological sites and central places. Current
1455 Anthropology 38, 86–88.

1456 O'Connell, J.F., Hawkes, K., Lupo, K., Blurton Jones, N., 2002. Male strategies and Plio-Pleistocene
1457 archaeology. Journal of Human Evolution 43, 831–872.

1458 O'Connell, J.F., Hawkes, K., Blurton Jones, N., 1992. Patters in the distribution, site structure and
1459 assemblage composition of Hadza kill-butchering sites. Journal of Archaeological Science 19,
1460 319–345.

1461 Olsen, S.L., Shipman, P., 1988. Surface modification on bone: trampling versus butchery. Journal of
1462 Archaeological Science 15, 535–553.

1463 Organista, E., Pernas-Hernández, M., Gidna, A., Yravedra, J., Domínguez-Rodrigo, M., 2016. An
1464 experimental lion-to-hammerstone model and its relevance to understand hominin-carnivore
1465 interactions in the archaeological record. Journal of Archaeological Science 66, 69–77.

1466 Owen, R.B., Renaut, R.W., Stamatakis, M.G., 2010. Diatomaceous sedimentation in late Neogene
1467 lacustrine basins of western Macedonia, Greece. Journal of Paleolimnology 44, 346-359.

Parker, A.G., 2009. Pleistocene climate change in Arabia: developing a framework for hominin dispersal over the last 350 ka. In: Petraglia, M.D., Rose, J. (Eds.), The Evolution of Human Populations in Arabia: Palaeoenvironments, Prehistory and Genetics. Springer, New York, pp. 39–49.

Parton, A., Farrant, A.R., Leng, M.J., Telfer, M.W., Groucutt, H.S., Petraglia, M.D., Parker, A.G., 2015a. Alluvial fan records from southeast Arabia reveal multiple windows for human dispersal. Geology 43, 295-298.

Parton, A., White, T.S., Parker, A.G., Breeze, P.S., Jennings, R., Groucutt, H.S., Petraglia, M.D., 2015b. Orbital-scale climate variability in Arabia as a potential motor for human dispersals. Quaternary International 382, 82–97.

Peters, J., Van Neer, W., Plug, I., 1997. Comparative postcranial osteology of hartebeest (*Alcelaphus buselaphus*), scimitar oryx (*Oryx dammah*) and addax (*Addax nasomaculatus*), with notes on the osteometry of gemsbok (*Oryx gazella*) and Arabian oryx (*Oryx leucoryx*). Annals des Sciences Zoologiques du Musée Royal de L'Afrique Centrale 280, 1–83.

Petraglia, M.D., Alsharekh, A., Breeze, P., Clarkson, C., Crassard, R., Drake, N.A., Groucutt, H.S., Jennings, R., Parker, A.G., Parton, A., Roberts, R.G., Shipton, C., Matheson, C., al-Omari, A., Veall, M.A., 2012. Hominin Dispersal into the Nefud Desert and Middle Palaeolithic Settlement along the Jubbah Palaeolake, Northern Arabia. PLoS ONE. 7(11): e49840.

Petraglia, M.D., Alsharekh, A.M., Crassard, R., Drake, N.A., Groucutt, H., Parker, A.G., Roberts, R.G., 2011. Middle Paleolithic occupation on a Marine Isotope Stage 5 lakeshore in the Nefud Desert, Saudi Arabia. Quaternary Science Reviews 30, 1555–1559.

Pickering, T.R., 2002. Reconsideration of criteria for differentiating faunal assemblages accumulated by hyenas and hominids. International Journal of Osteoarchaeology 12, 127–141.

Pickering, T.R., Egeland, C.P., 2006. Experimental patterns of hammerstone percussion damage on bones: implications for inferences of carcass processing by human. Journal of Archaeological Science 33, 459–469.

Pobiner, B.L., 2007. Hominin-carnivore interactions: evidence from modern carnivore bone modification and early Pleistocene archaeofaunas (Koobi Fora, Kenya; Olduvai Gorge, Tanzania). Ph.D. dissertation, The State University of New Jersey.

Price, G.J., 2008. Taxonomy and palaeobiology of the largest-ever marsupial, *Diprotodon* Owen, 1938 (Diprotodontidae, Marsupialia). Zoological Journal of the Linnean Society, 153, 369–397.

Renberg, I., Brodin, Y.W., Cronberg, G., Eldaoushy, F., Oldfield, F., Rippey, B., Sandoy, S., Wallin, J.E., Wik, M., 1990. Recent acidification and biological changes in Lilla-Öresjön, Southwest Sweden, and the relation to atmospheric-pollution and land-use history. Philosophical Transactions of the Royal Society of London Series B-Biological Sciences 327, 391-396.

Roberts, P., Stewart, M., Alagaili, A.N., Breeze, P., Candy, I., Drake, N., Groucutt, H.S., Scerri, E.M.L., Lee-Thorp, J., Louys, J., Zalmout, I.S., Al-Mufarreh, Y.S.A., Zech, J., Alsharekh, A.M., al Omari, A., Boivin, N., Petraglia, M.D., 2018. Fossil herbivore stable isotopes reveal Middle Pleistocene hominin palaeoenvironment in 'Green Arabia'. Nature Ecology and Evolution 2, 1871–1878.

Rodríguez-Alba, J.J., Linares-Matás, G., Yravedra, J., 2019. First assessments of the taphonomic behaviour of Jaguar (*Panthera onca*). Quaternary International (in press). doi: 10.1016/j.quaint.2019.05.004

Rosenberg, T.M., Preusser, F., Fleitmann, D., Schwalb, A., Penkman, K., Schmid, T.W., Al-Shanti, M.A., Kadi, K., Matter, A., 2011. Humid periods in southern Arabia: Windows of opportunity for modern human dispersal. Geology 39, 1115–1118.

Rosenberg, T.M., Preusser, F., Risberg, J., Plikk, A., Kadi, K.A., Matter, A., Fleitmann, D., 2013. Middle and Late Pleistocene humid periods recorded in palaeolake deposits of the Nafud desert, Saudi Arabia. Quaternary Science Reviews 70, 109–123.

RStudio Team, 2015. RStudio: Integrated Development for R. RStudio, Inc., Boston, MA URL http://www.rstudio.com

Sala, N., Arsuaga, J.L., Hayne, G., 2014. Taphonomic comparison of bone modification caused by wild and captive wolves (*Canis lupus*). Quaternary International 330, 126–135.

Schaller, G.B., 1972. The Serengeti Lion: A Study of Predator-Prey Relations. University of Chicago Press, Chicago.

Scerri, E.M.L., 2012. A new stone tool assemblage revisited: reconsidering the 'Aterian' in Arabia. Proceedings of the Seminar for Arabian Studies 42, 357–370.

Scerri, E.M.L., Breeze, P.S., Parton, A., Groucutt, H.S., White, T.S., Stimpson, C., Clark-Balzan, L., Jennings, R., Alsharekh, A.M., Petraglia, M.D., 2015. Middle to late Pleistocene human habitation in the western Nefud Desert, Saudi Arabia. Quaternary International 382, 200–214.

Scerri, E.M.L., Drake, N.A., Jennings, R., Groucutt, H.S., 2014a. Earliest evidence for the structure of *Homo sapiens* populations in Africa. Quaternary Science Reviews 101, 207–216.

1529 Scerri, E.M.L., Groucutt, H.S., Jennings, R.P., Petraglia, M.D., 2014b. Unexpected technological
1530 heterogeneity in northern Arabia indicates complex late Pleistocene demography at the gateway
1531 to Asia. Journal of Human Evolution 75, 125–142.

1532 Scerri, E.M.L., Shipton, C., Clark-Balzan, L., Frouin, M. Schwenninger, J.-L., Groucutt, H.S., Breeze,
1533 P.S., Parton, A., Blinkhorn, J., Drake, N.A., Jennings, R., Cuthbertson, P., al Omari, A.,
1534 Alsharekh, A.M., Petraglia, M.D., 2018. The expansion of later Acheulean hominins into the
1535 Arabian Peninsula. Scientific Reports 8, 17165.

1536 Schaller, G.B., 1972. The Serengeti Lion. University of Chicago Press, Chicago.

1537 Selvaggio, M.M., 1994. Carnivore tooth marks and stone tool butchery marks on scavenged bones:
1538 archaeological implications. Journal of human evolution 27, 215–228.

1539 Shipton, C., Parton, A., Breeze, P.S., Jennings, R., Groucutt, H.S., White, T.S., Drake, N., Crassard, R.,
1540 Alsharekh, A., Petraglia, M.D., 2014. Large Flake Acheulean in the Nefud Desert of Northern
1541 Arabia. PaleoAnthropology 446–462.

1542 Spinage, C.A., 1972. African ungulate life tables. Ecology 53, 645–652.

1543 Steele, T.E., 2004. Variation in mortality profiles of red deer (*Cervus elaphus*) in Middle Palaeolithic
1544 assemblages from western Europe. International Journal of Osteoarchaeology 14, 307–320.

1545 Stewart, M., Louys, J., Price, G.J., Drake, N.A., Groucutt, H.S., Petraglia, M.D., 2017. Middle and Late
1546 Pleistocene mammal fossils of Arabia and surrounding regions: Implications for biogeography
1547 and hominin dispersals. Quaternary International (in press). doi: 10.1016/j.quaint.2017.11.052.

1548 Stimpson, C.M., Breeze, P.S., Clark-Balzan, L., Groucutt, H.S., Jennings, R., Parton, A., Scerri, E.,
1549 White, T.S., Petraglia, M.D., 2015. Stratified Pleistocene vertebrates with a new record of a
1550 jaguar-sized pantherine (*Panthera* cf. *gombaszogensis*) from northern Saudi Arabia. Quaternary
1551 International 382, 168–180.

1552 Stimpson, C.M., Lister, A., Parton, A., Clark-Balzan, L., Breeze, P.S., Drake, N.A., Groucutt, H.S.,
1553 Jennings, R., Scerri, E.M.L., White, T.S., Zahir, M., Duval, M., Grün, R., Al-Omari, A., Al
1554 Murayyi, K.S.M., Zalmout, I.S., Mufarreh, Y.A., Memesh, A.M., Petraglia, M.D., 2016. Middle
1555 Pleistocene vertebrate fossils from the Nefud Desert, Saudi Arabia. Quaternary Science Reviews
1556 143, 13–36.

1557 Stiner, M.C., 1990. The use of mortality patterns in archaeological studies of hominid predatory
1558 adaptations. Journal of Anthropological Archaeology 9, 305–351.

1559 Stoermer, E.F., Edlund, M.B., Pilskaln, C.H., Schelske, C.L., 1995. Siliceous microfossil distribution

in the surficial sediments of Lake Baikal. Journal of Paleolimnology 14, 69–82.

Tappen, M., 1995. Savanna Ecology and Natural Bone Deposition. Current Anthropology 36, 223–260.

Tappen, M., Lordkipanidze, D., Bukshianidze, M., Ferring, R., Vekua, A., 2007. Are you in or out (of Africa)? Site formation at Dmanisi and actualistic studies in Africa. In: Pickering, T.R., Schick, K., Toth, N. (Eds.), Breathing Life Into Fossils: Taphonomic Studies in Honor of C.K. (Bob) Brain. Stone Age Institute Press, Gosport, Indiana, pp. 119–136.

Thomas, H., Geraads, D., Janjou, D., Vaslet, D., Memesh, A., Billiou, D., Bocherens, H., Dobigny, G., Eisenmann, V., Gayet, M., Lapparent de Broin, F., Petter, G., Halawani, M., 1998. First Pleistocene faunas from the Arabian peninsula: an Nafud desert, Saudi Arabia. Comptes Rendus de l'Académie des Sciences - Series IIA - Earth and Planetary Science 326, 145–152.

Turner, A., Anton, M., 1997. The Big Cats and their Fossil Relatives. Columbia University Press, New York.

Vaks, A., Bar-Matthews, M., Ayalon, A., Matthews, A., Halicz, L., Frumkin, A., 2007. Desert speleothems reveal climatic window for African exodus of early modern humans. Geology 35, 831–834.

Vaks, A., Bar-Matthews, M., Matthews, A., Ayalon, A., Frumkin, A., 2010. Middle-Late Quaternary paleoclimate of northern margins the Saharan-Arabian Desert: reconstruction from speleothems of Negev Desert, Israel. Quaternary Science Reviews 29, 2647–2662.

Villa, P., Mahieu, E., 1991. Breakage pattern of human long bones. Journal of Human Evolution 21, 27–48.

Voorhies, M.R., 1969. Taphonomy and population dynamics of an early Pliocene fauna, Knox County, Nebraska. University of Wyoming Contributions to Geology, Special Paper 1, 1–69.

Weaver, T.D., Boyko, R.H., Steele, T.E., 2011. Cross-platform program for likelihood-based statistical comparisons of mortality profiles on a triangular graph. Journal of Archaeological Science 38, 2420–2423.

Wickham, H., 2016. ggplot2: Elegant graphics for data analysis. Springer-Verlag, New York.

Wolverton, S., 2001. Caves, ursids, and artifacts: a natural-trap hypothesis. Journal of Ethnobiology 21, 55–72.

Yravedra, J., Domínguez-Rodrigo, M., Santonja, M., Pérez-González, A., Panera, J., Rubio-Jara, S., Baquedano, E., 2010. Cut marks on the middle Pleistocene elephant carcass of Áridos 2 (Madrid, Spain.

1590 Journal of Archaeological Science 37, 2469–2476.

Tables

Table 1. Species representation according to NISP and MNI for the Unit 5 and Elephant Quarry assemblages.

		Unit 5		EQ	Unit 5 + EQ
		NISP	**MNI**	**NISP**	**MNI**
Birds					
	Neoprhon percnopterus	5	1		1
	Pterocles orientalis	1	1		1
	Struthio sp.	2	1		1
	Tachybaptus sp.	1	1		1
	Milvus sp.	1	1		1
	Anas sp.	1	1		1
	Motacilla sp.	2	1		1
	Indet. birds	18		8	
	Total birds	**31**	**7**	**8**	**7**
Reptiles					
	Squamata	9	2	4	2
	Testudines	4	1	4	1
	Total reptiles	**13**	**3**	**8**	**3**
Mammals					
	Leporidae	1	1		1
	Rodentia	2	1		1
	cf. Mustelidae	1	1		1
	Vulpes sp	4	1	8	1
	Canis sp	4	1	1	2
	Panthera sp.	3	1		1
	Indet. carnivores	8		10	
	Small bovids	18	1	4	1
	Indet. small mammals	47		19	
	Total small mammals	**88**	**7**	**42**	**8**
	Alcelaphinae			2	1
	Oryx sp.	240	7	44	10
	Equus sp.	7	2	13	3
	Indet. medium mammals	115		34	
	Total medium mammals	**362**	**9**	**93**	**14**
	Camelidae	1	1	1	1
	Palaeoloxodon sp. cf. *P. recki*	17	2	114	4
	Indet. large mammals	3		4	
	Total large mammals	**21**	**3**	**119**	**5**
	Indet. mammals	87		60	
	Total	**602**	**29**	**330**	**37**

Table 2. Results of the Unit 5 taphonomic analysis broken down by size class ("% of" values refer to the %NISP for the specific bone portion).

		Small-sized animal	Medium-sized animal	Large-sized animal	Indet.-sized mammal	TOTAL
NRSP		/	/	/	/	1644
NISP		132	361	21	88	602
Weathering						
0	*n*	30	54	1	9	91
1	*n*	30	104	2	18	154
2	*n*	18	104	1	17	140
3	*n*	5	35	3	5	48
4	*n*	0	5	0	0	5
5	*n*	0	0	0	0	0
Breakage						
Green	*n*	4	35	/	4	43
Dry	*n*	3	30	/	1	34
Intermediate	*n*	5	7	/	0	12
Midshaft circumference						
Type 1	*n*	3	25	/	4	32
Type 2	*n*	3	11	/	0	14
Type 3	*n*	12	33	/	0	35
Carnivore gnawing						
Total	*n*	14	86	1	12	113
	%	10.6%	23.8%	4.8%	13.6%	18.7%
Epiphysis	*n*	4	16	0	0	20
	% of	22.2%	25.8%	0.0%	0.0%	24.4%
Midshaft	*n*	2	20	0	0	22
	% of	57.1%	23.8%	0.0%	0.0%	21.4%
Probable butchery marks						
Hammerstone(?)	*n*	0	3	0	0	3
	%	0.0%	0.8%	0.0%	0.0%	0.5%
Cut mark(?)	n	0	2	0	0	2
	%	0.0%	0.6%	0.0%	0.0%	0.3%
Rodent gnawing	*n*	0	2	0	0	2
	%	0%	0.6%	0%	0.0%	0.3%
Root etching	*n*	3	17	0	4	24
	%	2.3%	4.7%	0.0%	4.5%	4.5%
Staining (manganese)	*n*	0	3	0	0	3
	%	0.0%	0.8%	0.0%	0.0%	0.5%
Abrasion	*n*	1	7	0	0	8
	%	0.8%	1.9%	0.0%	0%	1.3%

Table 3. Results of the Unit 5 taphonomic analysis broken down by trench ("% of" values refer to the %NISP for the specific bone portion).

		Trench 1	Trench 2	Trench 4	Trench 5	Trench 6
NRSP		834	169	122	68	275
NISP		321	42	27	68	95
Weathering						
0	*n*	53	10	4	3	11
1	*n*	85	6	5	24	20
2	*n*	72	8	3	20	26
3	*n*	25	2	2	7	11
4	*n*	1	0	2	2	0
5	*n*	0	0	0	0	0
Breakage						
Green	*n*	20	2	3	6	6
Dry	*n*	13	0	0	13	5
Intermediate	*n*	5	0	0	1	3
Midshaft circumference						
Type 1	*n*	12	3	2	5	5
Type 2	*n*	7	0	0	3	2
Type 3	*n*	19	0	0	17	7
Carnivore gnawing						
Total	*n*	49	3	3	27	24
	%	15.3%	7.1%	11.1%	39.7%	25.7%
Epiphysis	*n*	5	0	0	9	5
	% of	13.9%	0.0%	0.0%	29.0%	55.6%
Midshaft	*n*	7	1	0	8	2
	% of	13.5%	20.0%	0.0%	33.3%	14.3%
Probable butchery marks						
Hammerstone(?)	*n*	3	0	0	0	0
	%	1.0%	0.0%	0.0%	0.0%	0.0%
Cut mark(?)	n	1	0	0	1	0
	%	0.3%	0.0%	0.0%	1.5%	0.0%
Rodent gnawing	*n*	1	0	0	1	0
	%	0.3%	0.0%	0.0%	1.5%	0.0%
Root etching	*n*	9	0	0	3	10
	%	2.9%	0.0%	0.0%	4.4%	10.5%
Staining (manganese)	*n*	2	0	0	1	0
	%	0.6%	0.0%	0.0%	1.5%	0.0%
Abrasion	*n*	4	0	0	2	2
	%	1.3%	0.0%	0.0%	2.9%	2.1%

1601 **Table 4.** Unit 5 Skeletal part representation according to NISP and MNE.

Element	Rodent, bird, and reptile		Carnivore		Small bovid		Medium bovid		Equid		Large animal (elephant, camel)		Indet. animal (sml / med / lge / indet.)
	NISP	MNE	NISP	MNE	NISP	MNE	NISP	MNE	NISP	MNE	NISP	MNE	NISP
Cranium	5	2	3	2	4	1	24	11	–	–	–	–	1 / 5 / – / 9
Horn core	–	–	–	–	–	–	7	3	–	–	–	–	– / – / – / –
Mandible (one side)	1	1	–	–	1	1	26	14	1	4	2	2	– / 3 / – / 2
Tooth	1	1	6	6	2	2	27	27	–	–	7	1	2 / 1 / – / 6
Atlas	–	–	–	–	–	–	4	4	–	–	–	–	– / 1 / – / –
Axis	–	–	–	–	–	–	5	5	–	–	–	–	– / – / – / –
Cervical vertebrae	1	1	–	–	–	–	8	8	–	–	–	–	– / 1 / – / 1
Thoracic vertebrae	–	–	3	3	–	–	8	8	4	4	3	3	1 / 2 / – / 2
Lumbar vertebrae	–	–	2	2	–	–	3	3	–	–	–	–	– / 1 / – / 1
Caudal vertebrae	–	–	1	1	–	–	–	–	–	–	–	–	– / – / – / 1
Indet. vertebrae	11	11	1	1	–	–	–	–	–	–	1	1	2 / 6 / – / –
Furcula / clavicle	2	2	–	–	–	–	–	–	–	–	–	–	– / – / – / –
Rib	2	1	–	–	–	–	22	2	–	–	1	1	15 / 44 / – / 22
Sacrum	2	2	1	1	–	–	3	2	–	–	–	–	2 / 1 / – / 2
Sternum	–	–	–	–	–	–	–	–	–	–	–	–	– / – / – / –
Scapula	1	1	–	–	2	2	13	4	–	–	–	–	5 / 3 / – / –
Pelvis	–	–	–	–	–	–	6	3	–	–	1	1	4 / – / – / 1
Humerus	8	5	–	–	3	2	6	4	–	–	–	–	4 / 1 / – / 1
- Complete	–		–		–		–		–		–		– / – / – / –
- Prox. ep.	–		–		–		–		–		–		1 / – / – / 1
- Pox. ep. + shaft	2		–		–		–		–		–		1 / – / – / –
- MSHF	1		–		3		2		–		–		1 / 1 / – / –
- Dist. ep. + shaft	3		–		–		3		–		–		– / – / – / –
- Dist. ep.	1		–		–		1		–		–		1 / – / – / –
Radius	1	1	1	1	1	1	6	5	–	–	–	–	– / 1 / – / 1
- Complete	1		–		–		3		–		–		– / – / – / –
- Prox. ep.	–		–		1		1		–		–		– / – / – / –
- Pox. ep. + shaft	–		1		–		1		–		–		– / 1 / – / –
- MSHF	–		–		–		–		–		–		– / – / – / 1
- Dist. ep. + shaft	–		–		–		–		–		–		– / – / – / –
- Dist. ep.	–		–		–		1		–		–		– / – / – / –
Ulna	1	1	–	–	–	–	7	7	–	–	–	–	– / 1 / – / 2

Metacarpal	–	–	1	1	1	1	11	9	–	–	–	–	– / – / – / –
- Complete	–		1		1		3		–		–		– / – / – / –
- Prox. ep.	–		–		–		1		–		–		– / – / – / –
- Pox. ep. + shaft	–		–		–		5		–		–		– / – / – / –
- MSHF	–		–		–		–		–		–		– / – / – / –
- Dist. ep. + shaft	–		–		–		2		–		–		– / – / – / –
- Dist. ep.	–		–		–		–		–		–		– / – / – / –
Femur	2	1	–	–	–	–	–	–	2	1	–	–	2 / 1 / – / 1
- Complete	–		–		–		–		–		–		– / – / – / –
- Prox. ep.	–		–		–		–		–		–		2 / – / – / 1
- Pox. ep. + shaft	–		–		–		–		1		–		– / – / – / –
- MSHF	–		–		–		–		–		–		– / 1 / – / –
- Dist. ep. + shaft	1		–		–		–		1		–		– / – / – / –
- Dist. ep.	–		–		–		–		–		–		– / – / – / –
Tibia	–	–	–	–	–	–	12	11	–	–	–	–	– / 2 / – / –
- Complete	–		–		–		2		–		–		– / 1 / – / –
- Prox. ep.	–		–		–		–		–		–		– / – / – / –
- Pox. ep. + shaft	–		–		–		1		–		–		– / – / – / –
- MSHF	–		–		–		–		–		–		– / 1 / – / –
- Dist. ep. + shaft	–		–		–		7		–		–		– / – / – / –
- Dist. ep.	–		–		–		2		–		–		– / – / – / –
Patella	–	–	–	–	–	–	1	1	–	–	–	–	– / 2 / – / –
Astragalus	–	–	–	–	1	1	4	4	1	1	–	–	– / – / – / –
Calcaneus	–	–	–	–	–	–	3	3	–	–	–	–	– / – / – / –
Carpal / tarsal	–	–	–	–	–	–	7	7	–	–	2	2	1 / 4 / – / –
Metatarsal	1	1	–	–	–	–	9	8	–	–	–	–	– / – / – / –
- Complete	1		–		–		2		–		–		– / – / – / –
- Prox. ep.	–		–		–		1		–		–		– / – / – / –
- Pox. ep. + shaft	–		–		–		5		–		–		– / – / – / –
- MSHF	–		–		–		–		–		–		– / – / – / –
- Dist. ep. + shaft	–		–		–		1		–		–		– / – / – / –
- Dist. ep.	–		–		–		–		–		–		– / – / – / –
Indet. metapodial	–	–	–	–	1	1	4	–	–	–	1	1	– / 1 / – / –
Indet. MSHF	7	–	–	–	–	–	1	–	–	–	–	–	5 / 31 / – / 5
Phalanges													
- Proximal	–	–	1	1	1	1	7	7	–	–	–	–	– / – / – / –
- Intermediate	–	–	–	–	–	–	4	4	–	–	–	–	– / – / – / –
- Distal	–	–	–	–	1	1	–	–	–	–	–	–	– / – / – / –

- Indet.	–	–	–	–	–	–	–	–	–	–	–	–	2 / – / – / –
Sesamoid	–	–	–	–	–	–	1	1	–	–	–	–	– / 1 / – / 1
Carapace / plastron	1	1	–	–	–	–	–	–	–	–	–	–	– / – / – / –
Unidentified	–	–	–	–	–	–	–	–	–	–	–	–	1 / 1 / 3 / 30
Total	**47**	**33**	**20**	**19**	**18**	**14**	**239**	**165**	**8**	**7**	**18**	**12**	**47 / 114 / 3 / 88**

1602

Table 5. Chi-squared test comparisons of shaft ratio (Type 2 + Type 3:Type 1) for the Unit 5, TSR, TLS, and experimental scenarios modelling carnivore primary and secondary access to carcasses [data from Marean et al. (2004) and Sala et al. (2014)].

	Shaft ratio	**Unit 5**	**TSR**	**TLS**
Unit 5	1.53	–	75.852 $p < 0.001$	159.8 $p < 0.001$
TSR	0.12	75.852 $p < 0.001$	–	22.481 $p < 0.001$
TLS	0.12	159.8 $p < 0.001$	22.481 $p < 0.001$	–
Hyena-only	0.13	70.21 $p < 0.001$	4.821 $p = 0.090$	27.661 $p < 0.001$
Hammerstone-only	0.44	13.794 $p < 0.001$	60.299 $p < 0.001$	102.010 $p < 0.001$
Hammerstone-hyena	0.15	79.433 $p < 0.001$	8.586, $p = 0.014$	34.497 $p < 0.001$
Wolf-only	1.73	0.003 $p = 0.958$	146.02 $p < 0.001$	233.37 $p < 0.001$

Table 6. Results of Pearson's and Spearman's tests for correlation between Unit 5 small- and medium-sized ungulate skeletal part representation, bone mineral density (BMD), and economic utility (SFUI). Data from Tables S3 and S4.

	Small-sized ungulate				**Medium-sized ungulate**			
	Pearson		**Spearman**		**Pearson**		**Spearman**	
	r	*p*	r_s	*p*	r	*p*	r_s	*p*
Bone mineral density (BMD)	0.283	0.129	0.259	0.167	0.543	0.002	0.592	<0.001
SFUI (low- and high-survival)	-0.077	0.707	-0.241	0.236	-0.336	0.094	-0.273	0.178
SFUI (high-survival only)	-0.573	0.137	-0.652	0.114	-0.673	0.067	-0.491	0.221

Table 7. Chi-squared and Fisher's exact test results comparing mortality profiles of the Unit 5 fossil assemblage with modern carnivore, ethnographic, and zooarchaeological mortality data.

	Unit 5 (all juvenile)	**Unit 5 (subadult juvenile)**
Lion	χ^2 =0.727	χ^2 = 0.657
	p = 0.695	p = 0.720
Leopard	p = 0.796	p = 0.638
Ambush predators	χ^2 = 0.535	χ^2 = 0.394
	p = 0.765	p = 0.877
Hyena	χ^2 = 3.947	χ^2 = 0.006
	p = 0.139	p = 0.997
African wild dog	p < 0.001	p = 0.695
Cursorial predators	χ^2 = 7.595	χ^2 = 0.016
	p = 0.022	p = 0.992
Wolf	p = 0.225	–
Modern human	p = 0.710	p = 0.795
Klasies River Mouth	χ^2 = 1.969	p = 0.850
	p = 0.374	
Bovid Hill	p = 0.788	–
Kanjera South	p = 0.344	p = 0.443
FLK *Zinj*	p = 0.582	p = 0.642

* mortality data used in the analysis was taken from various sources: lion (Mitchell et al., 1965; Schaller, 1972; Spinage, 1972); leopard (Mitchell et al., 1965); Hyena (Kruuk, 1972); African wild dog (Mitchell et al., 1965; Schaller, 1972); Wolf (Steele, 2004); modern human (Bunn and Gurtov, 2014); Klasies River Mouth (Bunn and Gurtov, 2014); Bovid Hill (Jenkins et al., 2017); Kanjera South (Oliver et al., 2018); FLK *Zinj* (Oliver et al., 2018).

Table 8: Basic typological composition of the Ti's al Ghadah lithic assemblages (% are shown in brackets and refer to the % of each category within each assemblage).

Assemblage	Flake	Broken flake	Levallois flake	retouched	Levallois core	Non-Levallois core	Chips/ chunks
TIL	5 (41.7%)	4 (33.3%)	2 (16.7%)	/	/	/	1 (8.3%)
TSR	7 (70%)	/	1 (10%)	/	/	1 (10%)	1 (10%)
TLS	68 (50.7%)	16 (11.9%)	19 (14.2%)	10 (7.5%)	7 (5.2%)	13 (9.7%)	1 (0.7%)

Table 9: Raw material composition of the Ti's al Ghadah lithic assemblages (% are shown in brackets and refer to the % of each category within each assemblage).

Assemblage	Chert	Ferruginous quartzite	Other quartzite	Quartz	Igneous
TIL	1 (8.3%)	9 (75.0%)	/	/	2 (16.7%)
TSR	3 (30%)	4 (40%)	3 (30%)	/	/
TLS	53 (39.6%)	46 (34.3%)	32 (23.9%)	3 (2.2%)	/

Table 10: Comparison of basic flake dimensions for each assemblage, only using complete, unretouched flakes. All measurements in mm. First three columns are for all complete flakes, right hand three columns are only for complete flakes over 20 mm, to allow comparability.

Assemblage	Flake mean length	Flake mean thickness	Flake mean width	Flake >20 mm mean length	Flake >20 mm mean thickness	Flake >20 mm mean width
TIL	31.2	12.2	26.4	31.7	12.2	26.4
TSR	43.6	14.3	33.9	48.1	15.9	36.9
TLS	30.6	10.4	28.0	32.6	10.8	28.6

Fig. 1. Location and stratigraphy of the Ti's al Ghadah site (TAG): (A) Location (red triangle) of Ti's al Ghadah within the western Nefud Desert, Saudi Arabia; (B) Oblique 3D view of the topography of the site (derived using a differential GPS), with key landscape units discussed in the text marked.

Fig. 2. Stratigraphic log of Ti's al Ghadah showing the sedimentology of exposed marls and sands at the site. The numbering of units follows that of Stimpson et al. (2016) where full descriptions of the sedimentology can be found. Additional units added here are the IL A and IL B ferruginous marls (discussed in text).

Fig. 3. Frequencies (%NISP) of taxonomic representation broken down by assemblage (Unit 5, Elephant Quarry), region (northern trenches, southern trenches), and trenches.

Fig. 4. Distribution of frequencies (%NISP) for each specimen size range broken down by assemblage (Unit 5, Elephant Quarry), region (northern trenches, southern trenches), trenches, and animal size class.

Fig. 5. Unit 5 frequencies (%NISP, %MNE) of skeletal part representation by body portion (crania, axial, forelimb, hindlimb, distal limb, and feet).

Fig. 6. Voorhies transport groups according the %NISP and tooth to vertebra ratio for the Unit 5, northern, and southern trench assemblages. The limited/no (blue) and strong (red) influence bounds are plotted from data taken from Behrensmeyer (1975).

Fig. 7. Weathering stage according to %NISP for the Unit 5, southern, and northern trenches, and broken down by animal size.

Fig. 8. Examples of bone surface modifications from Unit 5 (A–C, G) and TSR (D–F): (A) *Oryx* sp. metacarpal (TAG14/917) with large carnivore tooth puncture; (B) *Oryx* sp. distal tibia (TAG14/917) with large tooth puncture and surficial root etching on it's the shaft; (C) *Oryx* sp. distal humerus (TAG14/1522) with furrowed distal epiphysis and manganese staining on the its shaft; (D) cortical view of a medium-sized animal midshaft fragment (TSR/763) with curved, smooth, and oblique fracture pattern, large flake scar with accompanying ripple marks, and a single angled V-shaped and slightly curved groove with subtle shoulder effect reminiscent of a cut mark; (E) medium-sized animal midshaft fragment (TSR/unnumbered) with three large and arcuate notches with corresponding negative and cortical flake scars; (F) medium-sized animal midshaft fragment (TSR/7126) with a single arcuate notch with corresponding negative flake scar and impact flake on opposing fracture surface; (G) *Palaeoloxodon* sp. cf. *P. recki* rib (SGS-NEFUD-108) with several parallel and straight grooves reminiscent of cut marks. The two grooves on the right are comparatively deep and exhibit clear shoulder effect. Scale bars for A–F and G are 20 mm and 20 cm, respectively.

Fig. 9. Frequency of tooth-marked medium-sized animal long bones, midshaft fragments, and epiphyses compared to the mean and 95% CI for experimental scenarios modelling: hyena primary access to carcasses (HI; Blumenschine, 1995); hyena secondary access to defleshed whole limb bones (WBH; Capaldo, 1997); hyena secondary access to defleshed and

demarrowed bones (HHI, HHII; Blumenschine, 1995; Capaldo, 1997); wild lion primary access to small/medium- (LI) and large-sized (LII) animals (Gidna et al., 2014); and hominin secondary access to carcasses following processing by lions (LH; Organista et al., 2016). Asterix (*) denotes samples that do not include metapodials.

Fig. 10. Ternary graphs comparing the mortality profile for medium-sized animals at Unit 5 to those killed by various carnivores (A, D), ambush (lions, leopards) and cursorial (hyenas, cheetahs, wild dogs) predators (B, E), and data taken from ethnographic and zooarchaeological contexts (C, F). Graphs on the left-hand side (A, B, C) include all individuals, whereas graphs on the right-hand side (D, E, F) exclude young juveniles. Ellipses approximate 95% confidence (CI) intervals. Shaded regions represent different mortality profile structures as defined by Stiner (1990) and discussed in the text: dark green, juvenile dominated; light green, attritional/U-shaped mortality profile; light brown, catastrophic/living structure; dark brown, prime-age dominated; white, old-age dominated. Sources for mortality data are provided in Table 7.

Figure 1

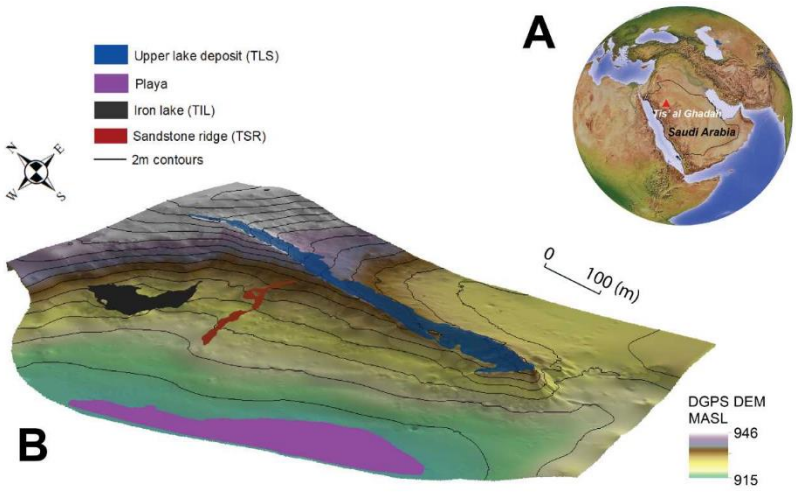
A
Upper lake deposit (TLS)
Playa
Iron lake (TIL)
Sandstone ridge (TSR)
2m contours
N
E
S
W
Tis' al Ghadah
Saudi Arabia
0
100 (m)
B
DGPS DEM
MASL
946
915

Figure 2

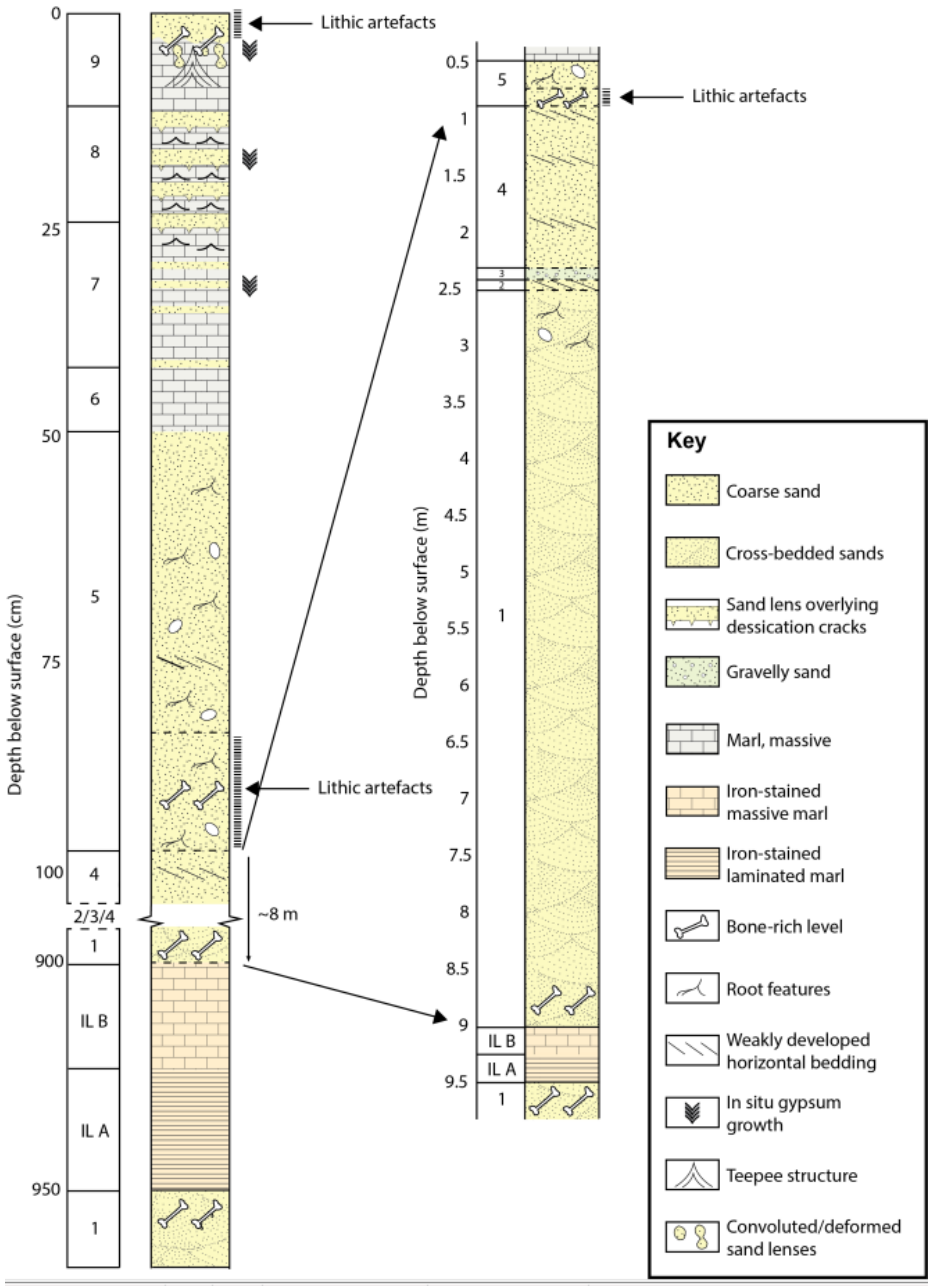
Lithic artefacts
Lithic artefacts
Lithic artefacts
~8 m
Depth below surface (cm)
Depth below surface (m)
0
25
50
75
100
900
950
9
8
7
6
5
4
2/3/4
1
IL B
IL A
1
0.5
1
1.5
2
2.5
3
3.5
4
4.5
5
5.5
6
6.5
7
7.5
8
8.5
9
9.5
Key
Coarse sand
Cross-bedded sands
Sand lens overlying dessication cracks
Gravelly sand
Marl, massive
Iron-stained massive marl
Iron-stained laminated marl
Bone-rich level
Root features
Weakly developed horizontal bedding
In situ gypsum growth
Teepee structure
Convoluted/deformed sand lenses

1751 **Figure 3**

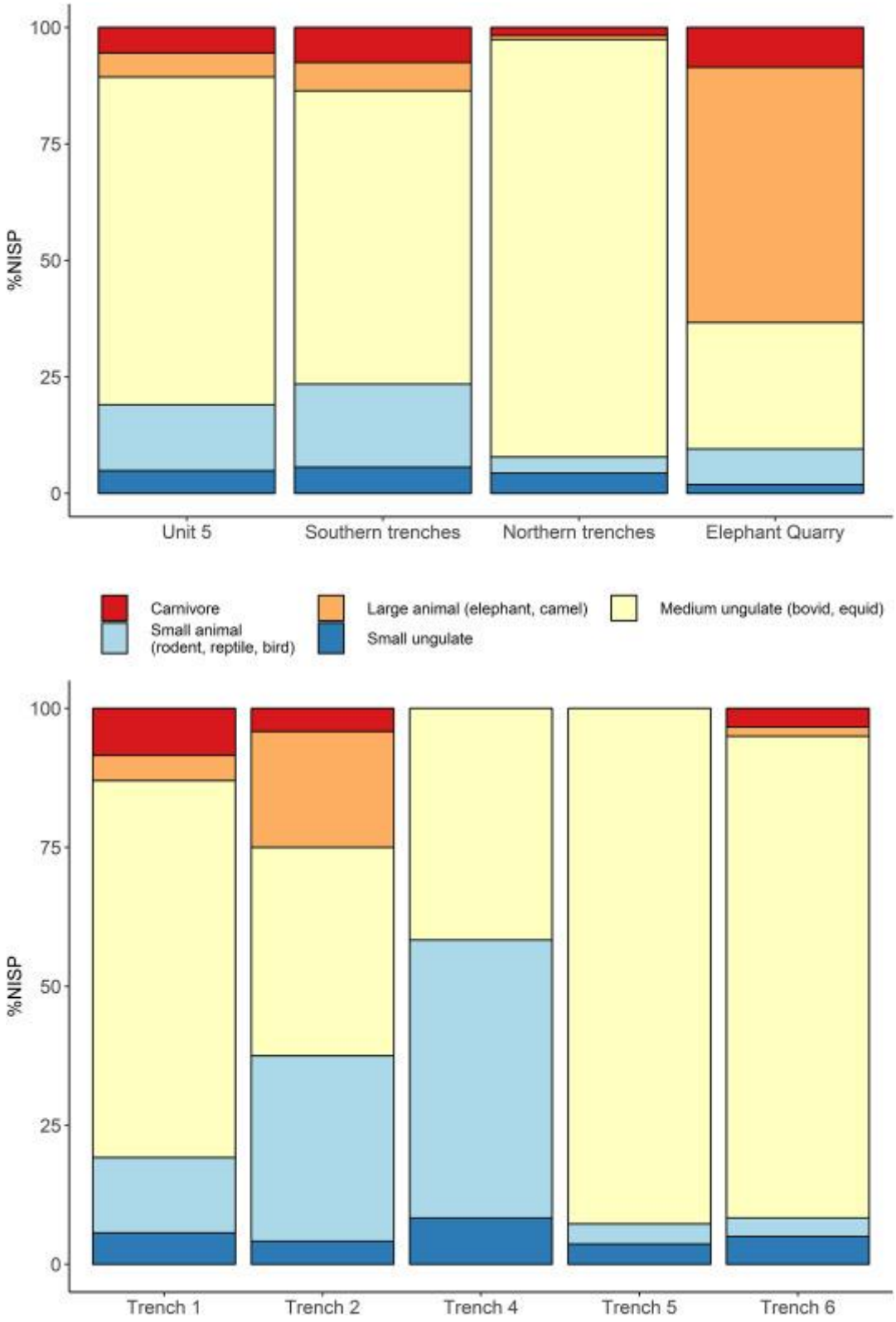

1752

1753

1754

1755

Figure 4

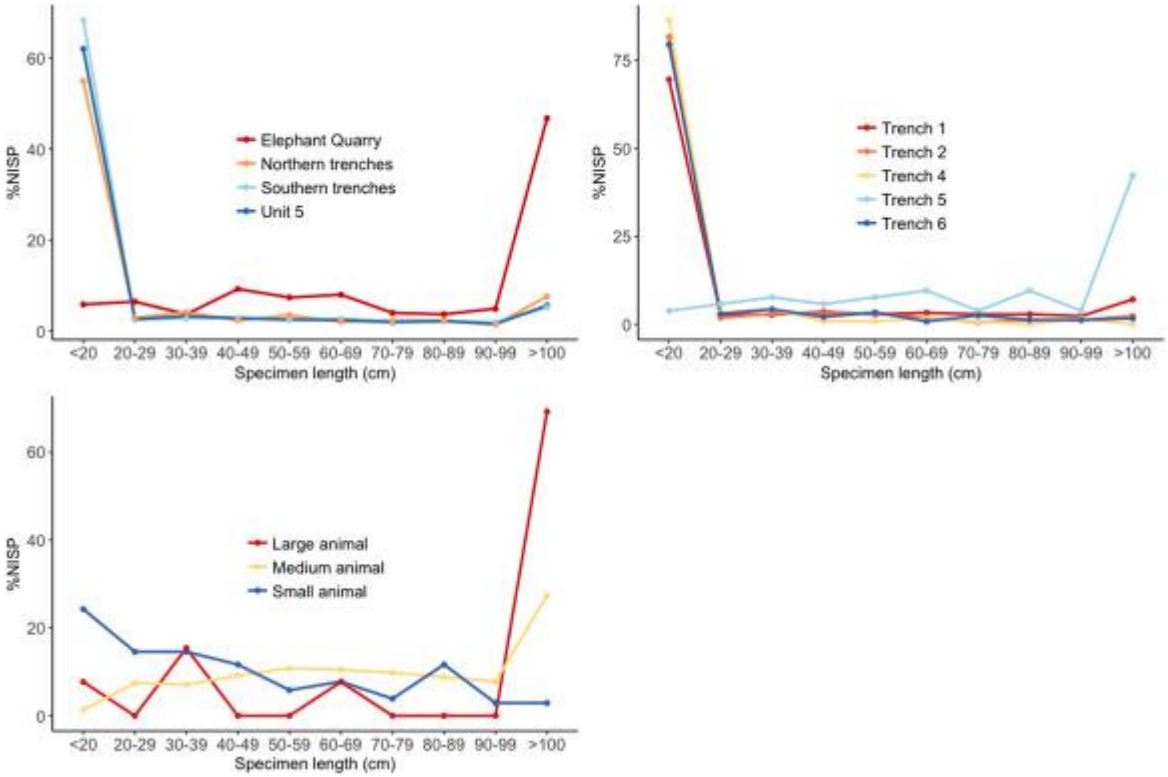
%NISP
Specimen length (cm)
<20 20-29 30-39 40-49 50-59 60-69 70-79 80-89 90-99 >100
Elephant Quarry
Northern trenches
Southern trenches
Unit 5
Trench 1
Trench 2
Trench 4
Trench 5
Trench 6
Large animal
Medium animal
Small animal

1772 **Figure 5**

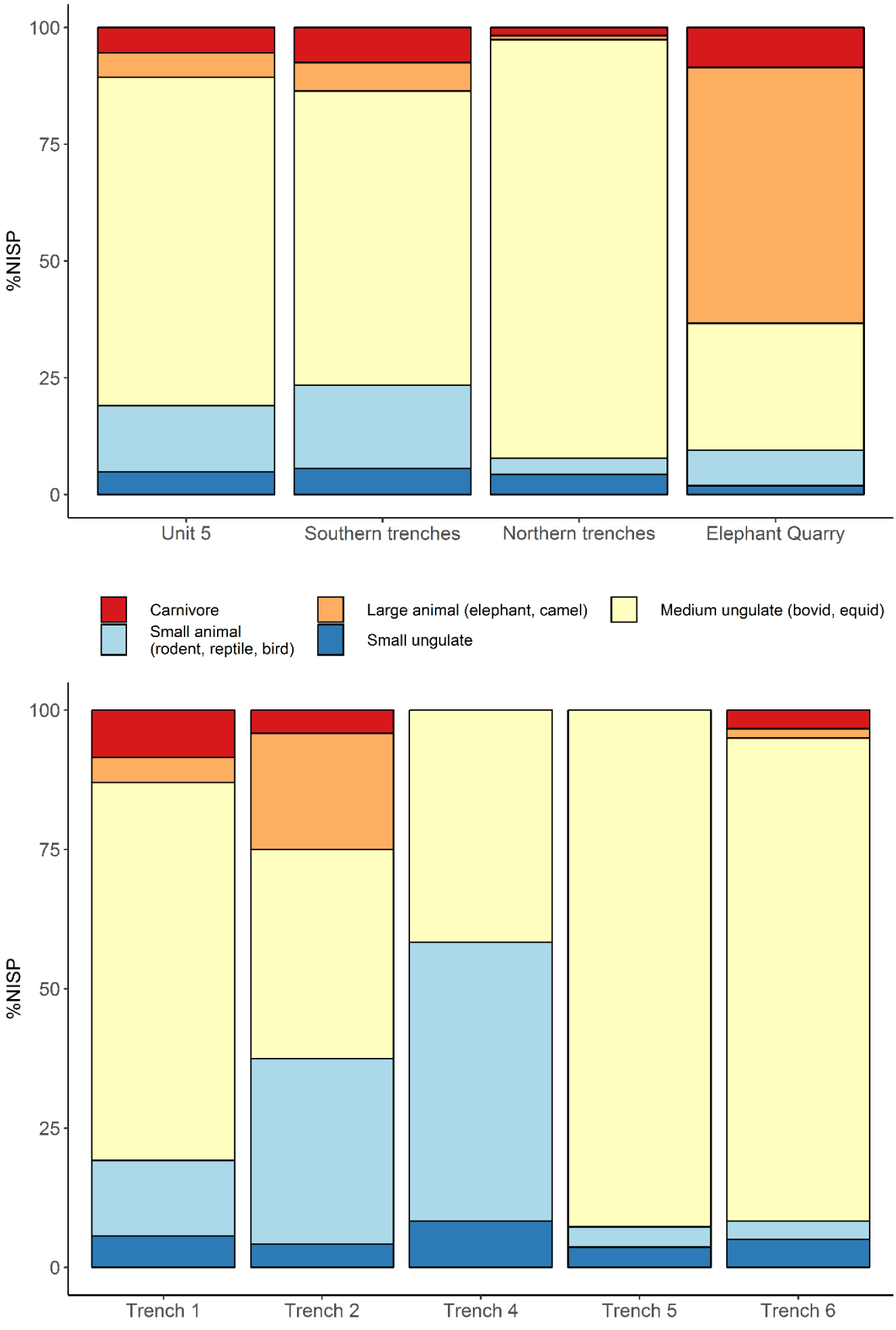

1773

Figure 6

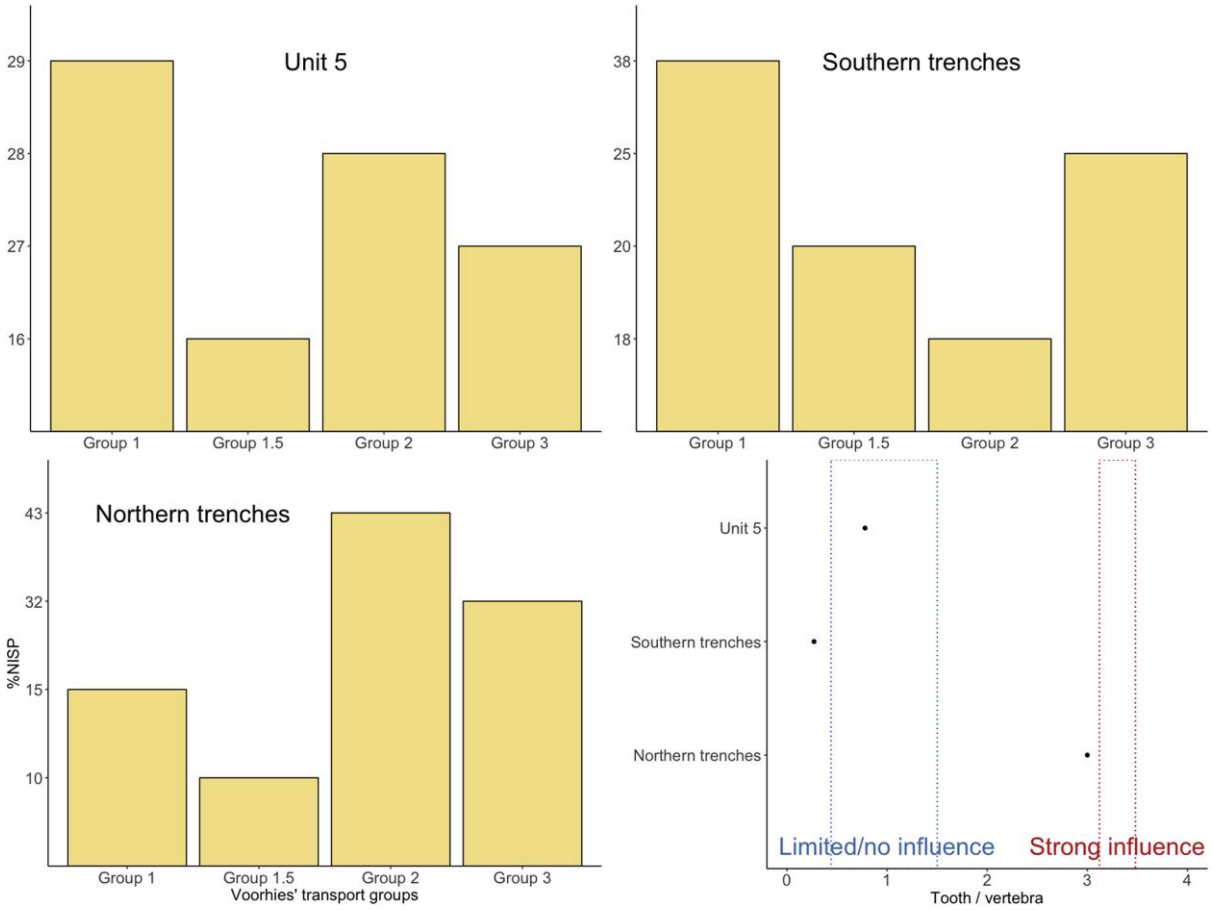
Unit 5
Southern trenches
Northern trenches
%NISP
Voorhies' transport groups
Group 1
Group 1.5
Group 2
Group 3
Unit 5
Southern trenches
Northern trenches
Limited/no influence
Strong influence
Tooth / vertebra

Figure 7

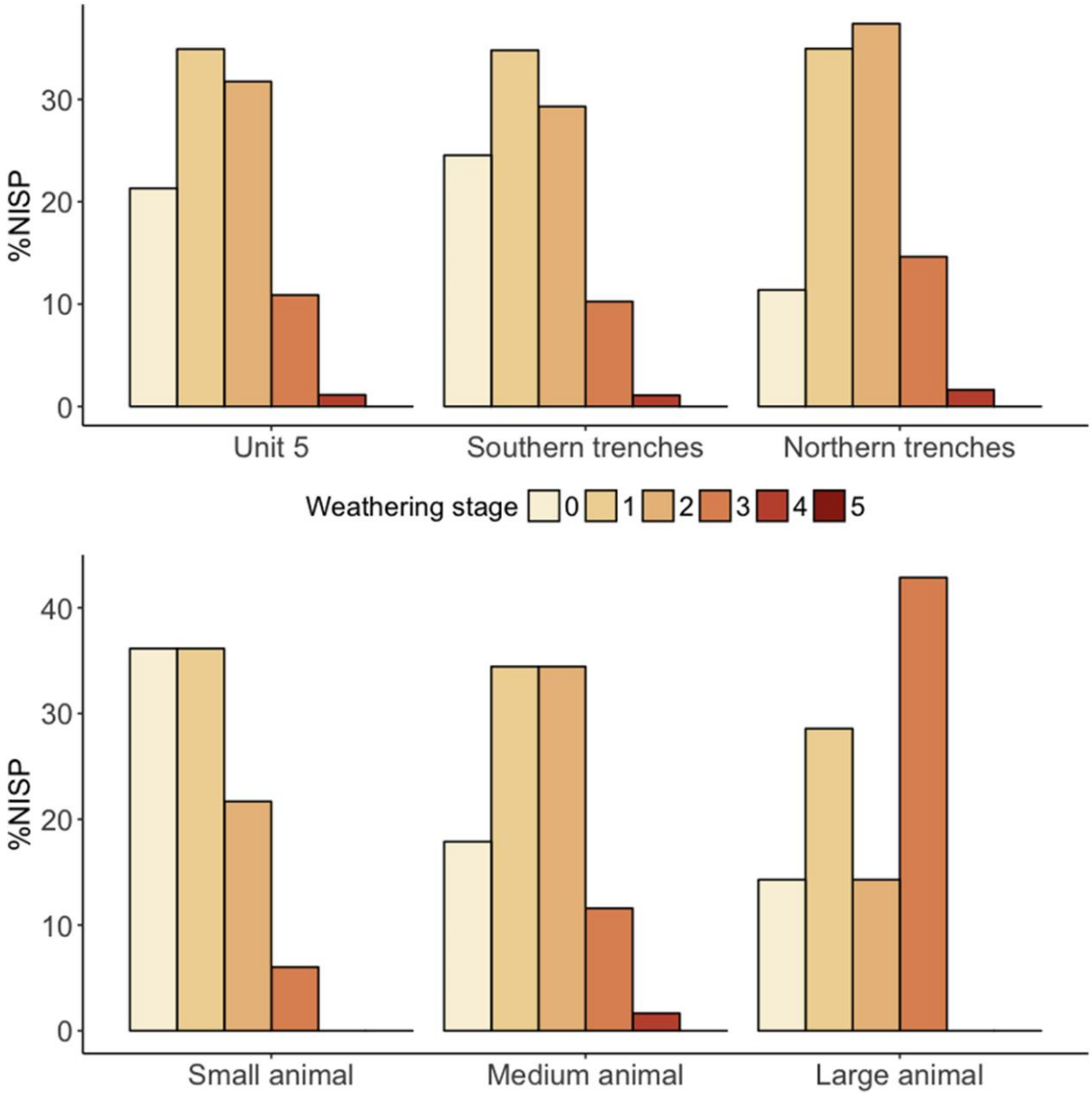
%NISP
30
20
10
0
Unit 5
Southern trenches
Northern trenches
Weathering stage 0 1 2 3 4 5
%NISP
40
30
20
10
0
Small animal
Medium animal
Large animal

Figure 8

Figure 9

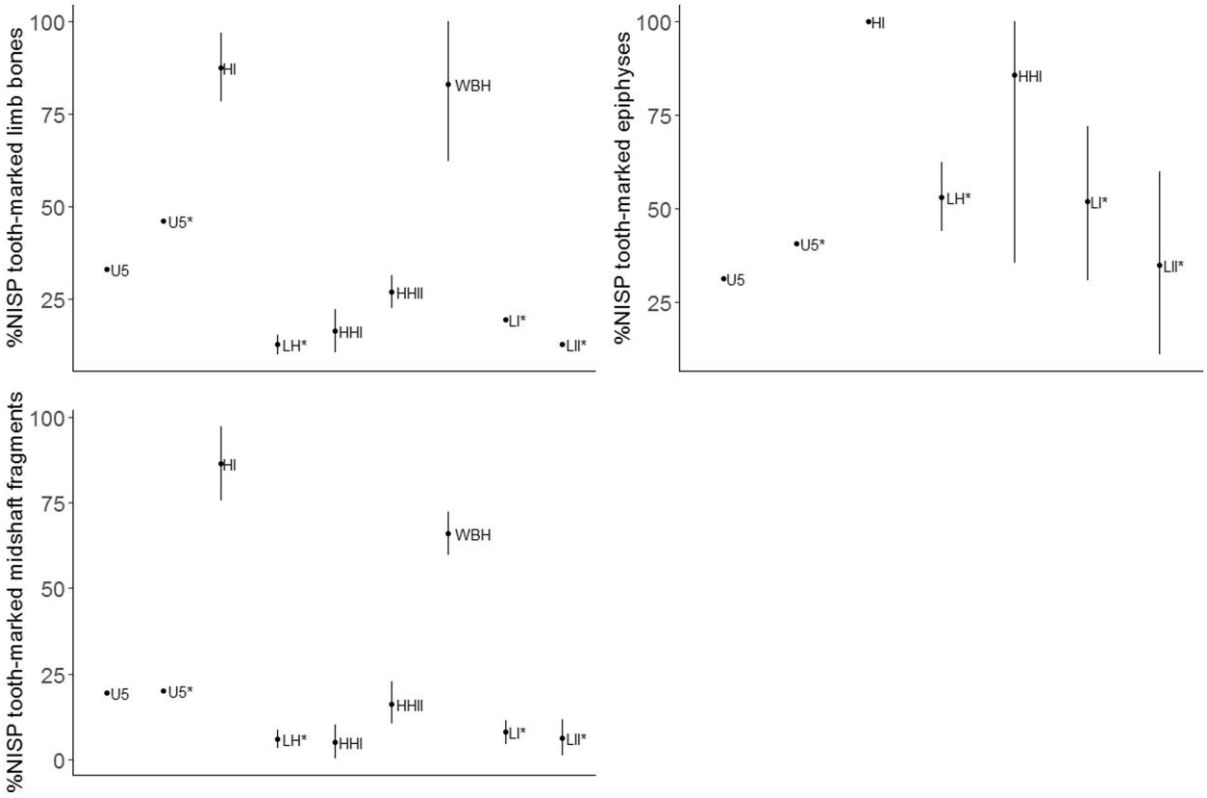
%NISP tooth-marked limb bones
100
75
50
25
U5
U5*
HI
LH*
HHI
HHII
WBH
LI*
LII*
%NISP tooth-marked epiphyses
100
75
50
25
U5
U5*
HI
LH*
HHI
LI*
LII*
%NISP tooth-marked midshaft fragments
100
75
50
25
0
U5
U5*
HI
LH*
HHI
HHII
WBH
LI*
LII*

Figure 10

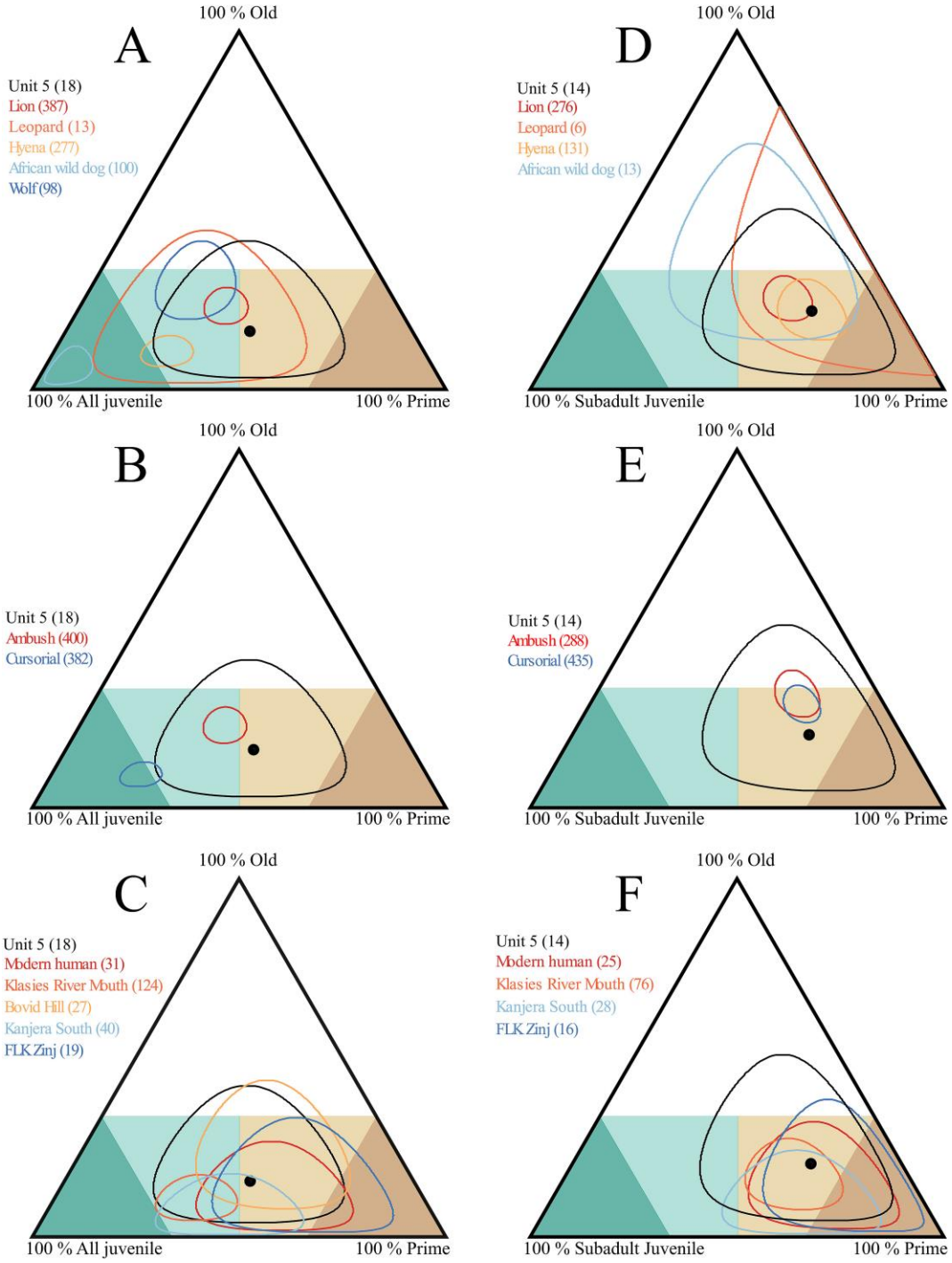
A
100 % Old
Unit 5 (18)
Lion (387)
Leopard (13)
Hyena (277)
African wild dog (100)
Wolf (98)
100 % All juvenile
100 % Prime
D
100 % Old
Unit 5 (14)
Lion (276)
Leopard (6)
Hyena (131)
African wild dog (13)
100 % Subadult Juvenile
100 % Prime
B
100 % Old
Unit 5 (18)
Ambush (400)
Cursorial (382)
100 % All juvenile
100 % Prime
E
100 % Old
Unit 5 (14)
Ambush (288)
Cursorial (435)
100 % Subadult Juvenile
100 % Prime
C
100 % Old
Unit 5 (18)
Modern human (31)
Klasies River Mouth (124)
Bovid Hill (27)
Kanjera South (40)
FLK Zinj (19)
100 % All juvenile
100 % Prime
F
100 % Old
Unit 5 (14)
Modern human (25)
Klasies River Mouth (76)
Kanjera South (28)
FLK Zinj (16)
100 % Subadult Juvenile
100 % Prime